Tensor Network Structure Search Via Canonical Dimension Tree Enumeration

Anonymous authors
Paper under double-blind review

Abstract

Tensor networks provide a powerful framework for compressing multi-dimensional data. The optimal tensor network structure for a given data tensor depends on both data characteristics and specific optimality criteria, making tensor network structure search a challenging problem. Existing solutions typically rely on sampling and compressing numerous candidate structures; these procedures are computationally expensive and therefore limiting for practical applications. We address this challenge by decoupling topology enumeration from rank assignment search. We first represent the search space using canonical dimension trees, a hierarchical structure that encodes potential network topology through nested index partitions. This representation inherently rules out redundant and suboptimal topologies by construction. To eliminate the assessment bottleneck, we introduce a mechanism powered by the precomputation of a singular value map. By archiving the singular values of all feasible tensor matricizations, we transform the evaluation of any candidate dimension tree into a constraint-solving problem. This allows us to solve for the near-optimal ranks and calculate the dimension tree's cost via simple metadata lookup, bypassing the on-the-fly tensor decompositions for all but the most promising candidates. Experimental results show that our approach improves search speed by up to 10× and achieves compression ratios 1.5× to 3× better than state-of-the-art. Notably, our approach scales to larger tensors that are unattainable by prior work. Furthermore, the discovered topologies generalize well to similar data; they achieve compression ratios up to 2.4× better than generic structures, while maintaining a search time of approximately 110 seconds for 6D tensors of 1–2 GB disk size.

1 Introduction

Tensor networks have found widespread applications in machine learning Lebedev et al. (2014); Novikov et al. (2015); Phan et al. (2020); Memmel et al. (2022); Sprangers & Vannieuwenhoven (2023), scientific computing Richter et al. (2021); Evenbly (2017); Gray & Chan (2024); Ma et al. (2024); Ceruti et al. (2021); Rakhuba (2021); Zhang & Kileel (2023), quantum computing Verstraete et al. (2008); Bañuls (2023); Montangero (2018); Arad & Landau (2010), among many other fields, because they allow effective low-rank approximations of high-dimensional data. Over the past decade, various tensor network structures—such as tensor trains (TT) Oseledets (2011), Tuckers Tucker (1966), and hierarchical Tuckers (HT) Grasedyck (2010)—have been deployed. Each of these structures offers distinct advantages for specific scenarios, with no single optimal representation across problem settings. This observation brings up an important question: given a data tensor and an optimization objective, how could one efficiently determine the most suitable tensor network structure to achieve the desired goal? This question has evolved into a research topic known as tensor network structure search (TN-SS).

TN-SS has two highly inter-related components: (1) the identification of a graph where nodes correspond to tensors and edges represent shared dimensions between connecting tensors; and (2) an assessment of the compression and approximation quality of each graph. More specifically, the task of searching for optimal tensor network structures involves two subtasks: (1) topology search: identify the optimal connections between nodes; and (2) rank search: find the optimal dimension sizes (also called ranks) for edges. While this division provides a clear framework to address the TN-SS problem, existing approaches face significant

challenges in effectively solving these subtasks. We categorize these problems into two primary challenges: the combinatorial explosion of the search space, and the prohibitive computational cost of candidate evaluation.

The first challenge is the vast search space to jointly optimize tensor network topology and ranks. A large portion of prior work has simplified this problem by focusing exclusively on either topology optimization with fixed ranks Li & Sun (2020); Hikihara et al. (2023); Haberstich et al. (2023) or rank optimization for a fixed topology Rai et al. (2014); Mickelin & Karaman (2020); Sedighin et al. (2021); Yin et al. (2022); Ghadiri et al. (2023). However, such isolated optimization often fails to identify the optimal structure where topology and rank are tightly coupled. Recent advancements attempt to address both subtasks simultaneously by sampling candidate structures from the joint search space Hashemizadeh et al. (2020); Li et al. (2022; 2023); Zeng et al. (2024); Zheng et al. (2024). However, the required sample size grows rapidly with the data tensor size, leading to a large number of candidates. The scalability issue is further exacerbated by the introduction of internal nodes, which enhances tensor network compression performance but can be inserted anywhere within tensor networks, exponentially increasing the topological search space. While greedy heuristics have been proposed to mitigate this explosion Hashemizadeh et al. (2020), they often sacrifice global optimality for computational feasibility, leaving the discovery of near-optimal structures an open problem.

Orthogonal to the search space explosion is the high overhead associated with candidate assessment. To determine the quality of a proposed structure, one must typically check whether the given data tensor can be compressed into this structure within the prescribed error tolerance. Standard techniques, such as alternating least squares Kolda & Bader (2009); Hashemizadeh et al. (2020) or gradient descent Kolda & Hong (2020); Li & Sun (2020); Li et al. (2022), involve iterative and computationally expensive tensor operations. When these assessment procedures are embedded into a large search loop, where thousands of candidates must be evaluated, the total search cost becomes prohibitive. Consequently, these is a critical need for more efficient assessment proxies that can accurately rank candidates.

1.1 Efficient TN-SS via Canonical Dimension Tree Enumeration

In this work, we propose a framework that decouples the topology and rank search, which is fundamentally different from prior work that attempt to sample the joint space of topologies and ranks. Instead, we enumerate topological skeletons represented by dimension trees, and then utilize a constraint-solving method to simultaneously solve for near-optimal ranks and evaluate candidate quality.

To achieve this decoupling, we first establish a representation of the network topology as a *canonical dimension tree*. A significant limitation of existing TN-SS methods is the redundant enumeration of network topologies alongside rank configurations. In contrast, we focus the search strictly on the skeleton level, defined as the graph connectivity and index placement without assigned edge weights. This enumeration is enabled by canonical dimension trees, which extends the dimension trees in classical tree tensor networks Falcó et al. (2021); Grasedyck (2010) by allowing multiple free indices to be assigned to both leaf and non-leaf nodes, but enforces every tensor network to be in canonical form. This presentation defines the search space through hierarchical index partitions. By treating the network topology as a nested set of partitions, we can systematically explore node connectivity with different free index placements. The structural constraints defined in canonical dimension trees naturally prune the search space, excluding duplicate enumeration and suboptimal topologies as they cannot be expressed as a valid dimension tree.

Complementing this structured search space, we introduce a constraint-solving framework as the primary engine for both candidate assessment and rank optimization. Traditionally, TN-SS algorithms treat ranks as discrete parameters to be sampled, and assessment as an expensive post-hoc factorization step. We replace this step inside the search loop with a calculation powered by a precomputed metadata map Ω that archives the singular values of the data tensor across all possible index bipartitions. Specifically, we leverage Ω to retrieve the approximated singular values and compute the truncation error for each edge (corresponds to tensor unfoldings) in a candidate dimension tree. This allows us to solve for the near-optimal rank assignment required to satisfy an error bound ε without performing live decompositions. These derived ranks are then used to calculate the tree's total size, which serves as the cost for the candidate dimension tree. We demonstrate that the size calculated through this method provides a rigorous over-approximation of the optimal size for a given topology. By replacing tensor decomposition with constraint

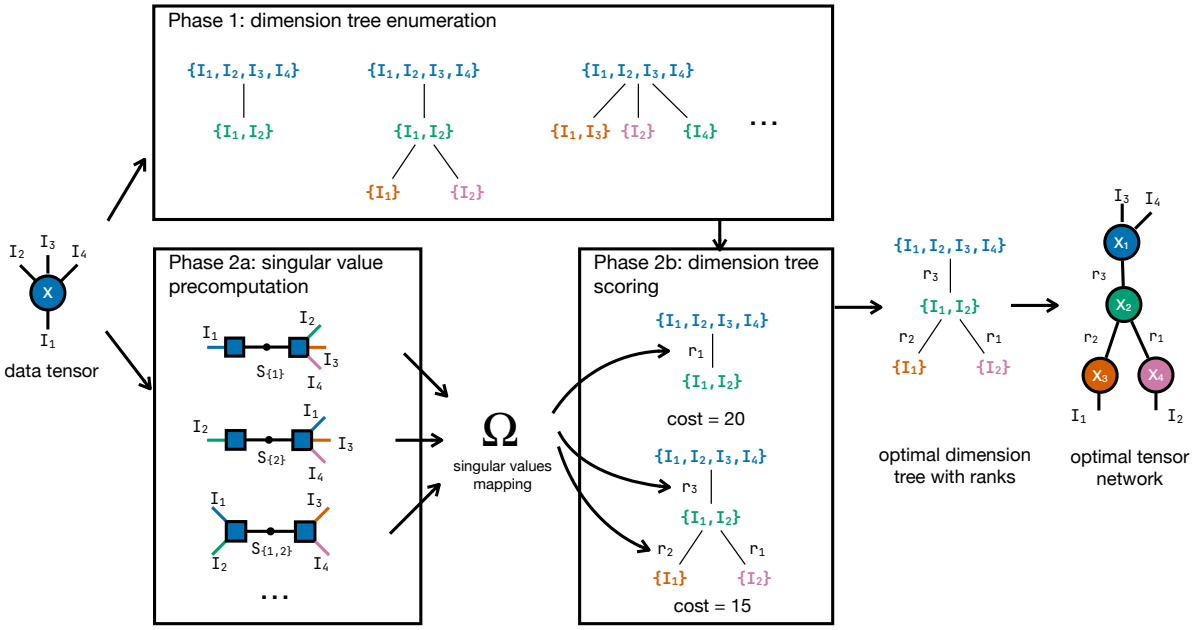

Figure 1: Overview of the proposed algorithm CADET. This algorithm consists of two phases: (1) enumeration of dimension trees, each representing a tensor network skeleton, and (2) scoring of dimension trees. The second phase includes two steps: (2a) pre-computation of singular values for all matricizations of the input tensor, and (2b) scoring of dimension trees without explicit decomposition. After the promising dimension trees are identified, tensor decomposition is run to obtain the optimal structure.

solving, our framework can identify near-optimal dimension trees and their corresponding rank assignments with significantly reduced computational overhead.

Synthesizing these components into a unified pipeline, the integrated workflow illustrated in Fig. 1 consists of two primary phases: dimension tree enumeration and constraint-based candidate scoring. First, the algorithm generates a collection of generalized dimension trees, each standing for a tensor network skeleton. Due to the special design of generalized dimension trees, this phase rules out suboptimal skeletons from the search space. It also significantly reduces the search space size by ignoring rank enumerations. Second, for each dimension tree, the algorithm queries the singular value map Ω to solve the rank optimization problem. The resulting rank assignment is used to calculate the tree size as the score, which effectively ranks the skeletons based on their estimated compression performance under the error constraint. By delaying computationally intensive tensor decompositions until the most promising skeletons and their ranks are determined, our strategy identifies high-performance network structures with the cost much lower than the traditional computational overhead.

Contributions In summary, we make the following contributions in this paper:

- We introduce canonical dimension trees to represent tensor network topologies. This representation encodes network topologies as hierarchical index partitions, and inherently rules out suboptimal and redundant skeletons by construction, effectively regularizing the search space (Section 3.2).
- We propose a novel evaluation mechanism that bypasses the need for full tensor compressions during the search phase. By formulating rank assignment as a constraint-solving problem over precomputed singular values, we can simultaneously optimize bond dimensions and assign quality scores to skeletons with low computational overhead (Section 3.3).
- We implement the proposed ideas as a tool named CADET (CAnonical DimEnsion Trees). We demonstrate the effectiveness of CADET through empirical evaluations and show that CADET runs significantly faster, achieves better compression ratios, and scales to larger tensors that baselines

cannot handle. Additionally, the discovered topologies can be generalized to unseen data from the same source (Section 5).

1.2 Related Work

Tensor Network Structure Search TN-SS has been explored in prior work from different aspects. Some studies Rai et al. (2014); Mickelin & Karaman (2020); Sedighin et al. (2021); Yin et al. (2022); Ghadiri et al. (2023) focus on optimizing rank assignments for specific tensor network topologies, proposing efficient algorithms to enumerate rank assignments against error constraints. Others focus on topology search with fixed internal ranks Li & Sun (2020); Hashemizadeh et al. (2020); Hikihara et al. (2023); Haberstich et al. (2023). Recent work Li et al. (2022; 2023); Zheng et al. (2024); Zeng et al. (2024) addresses the complete TN-SS problem by integrating topology and rank search, which often uses sampling-based methods and verifies if sampled structures satisfy error bounds. Zheng et al. Zheng et al. (2024) introduce an alternative, which encodes topology and rank search into a single optimization problem, and they solve this problem with the alternating direction method of multipliers. Our approach evolves traditional sampling-based methods by decoupling topology and rank search. We utilize canonical dimension trees to prune redundant candidates and a constraint-based scoring framework to accelerate candidate assessment. As demonstrated in Section 5.2, these strategies allow our method to identify structures with superior compression performance in significantly less search time than these baselines.

Low-Rank Tensor Decomposition Low-rank tensor decomposition has been studied for many different structures. Tucker decomposition Tucker (1966); De Lathauwer et al. (2000); Minster et al. (2020); Sun et al. (2020) factorizes a high-order tensor into a core tensor with several low-rank tensors, one for each mode. Tensor train decomposition Oseledets (2011); Aksoy et al. (2024) expresses a high-order tensor as a linear multiplication of 3-order tensors. Hierarchical Tucker decomposition Hackbusch & Kühn (2009); Grasedyck (2010); Falcó et al. (2021) generalizes tensor trains and tuckers to arbitrary trees, offering greater flexibility and compression potential. Beyond tree-based structures, several prior work Zhao et al. (2016); Handschuh (2015); Espig et al. (2012); Mickelin & Karaman (2020); Yang et al. (2017) explores cyclic structures, such as tensor rings or tensor chains. In contrast, our work focuses on searching for the optimal tree structure to compress the input data tensor. Cyclic structures are left as future work.

Tree Generation The systematic generation of tree structures is a foundational problem in enumerative combinatorics, governed by the growth patterns of Catalan and Schr"oder numbers Knuth (1997); Stanley (2015). Established algorithms for the exhaustive enumeration of these structures typically focus on the Constant Amortized Time (CAT) generation of non-isomorphic unlabeled trees using lexicographical sequences Aho & Hopcroft (1974); Beyer & Hedetniemi (1980); Zaks (1980); Erdős & Székely (1989); Sawada (2006); Kobayashi et al. (2025). In computational biology, these principles are adapted to model hierarchical complexity, such as in phylogenetics, where trees represent evolutionary lineages inferred from genetic data Semple et al. (2003); Wirtz (2022); Johnson (2012). Our work on dimension tree enumeration builds upon these combinatorial foundations but introduces a canonical form specialized for tensor network skeletons. Because tensor networks are inherently unrooted trees, they can be represented by multiple distinct rooted trees; our framework resolves this redundancy by defining a unique representative for each isomorphism class. This symmetry-breaking approach effectively prunes the search space.

2 Preliminaries

Definition 2.1 (Tensor, Tensor Size)**.** Let $d \in \mathbb{N}$ and $n_1, n_2, \ldots, n_d \in \mathbb{N}$. A tensor $\mathcal{X} \in \mathbb{R}^{n_1 \times n_2 \times \cdots \times n_d}$ is a d-dimensional array. The μ^{th} dimension of $\mathcal{X}$ has a name I_μ with size n_μ for all $\mu \in \{1, 2, \ldots, d\}$. The size of the tensor $\mathcal{X}$ is defined as $\texttt{size}(\mathcal{X}) = \prod_{\mu=1}^{d} n_\mu$.

Definition 2.2 (Matricization)**.** For a d-dimensional tensor $\mathcal{X} \in \mathbb{R}^{n_1 \times n_2 \times \cdots \times n_d}$ with indices $\{I_1, \ldots, I_d\}$, let $\pi_1, \pi_2, \ldots \pi_d$ be a permutation of $1, 2, \ldots, d$. We partition the dimensions of $\mathcal{X}$ into $\mathcal{I}_s = \{I_{\pi_1}, \ldots, I_{\pi_k}\}$ and $\overline{\mathcal{I}}_s = \{I_{\pi_{k+1}}, \ldots, I_{\pi_d}\}$ such that $\mathcal{I}_s \cap \overline{\mathcal{I}}_s = \emptyset$ and $\mathcal{I}_s \cup \overline{\mathcal{I}}_s = \{I_1, I_2, \ldots, I_d\}$. The $\mathcal{I}_s$-*matricization* of $\mathcal{X}$ is

$$\mathcal{X}^{(\mathcal{I}_s)} = \mathcal{X}(i_{\pi_1}, \ldots, i_{\pi_k}; i_{\pi_{k+1}}, \ldots, i_{\pi_d}) \tag{1}$$

In other words, indices in $\mathcal{I}_s$ enumerate the rows of $\mathcal{X}^{(\mathcal{I}_s)}$, and the remaining indices enumerate the columns.

Definition 2.3 (Tensor Contraction, Decomposition, and Truncated Decomposition)**.** The contraction between two tensors $\mathcal{A} \in \mathbb{R}^{n_1 \times n_2 \times \cdots \times n_\mu}$ and $\mathcal{B} \in \mathbb{R}^{n_\mu \times n_{\mu+1} \times \cdots \times n_d}$ along the μ^{th} dimension of $\mathcal{A}$ and first dimension of $\mathcal{B}$ is an operation represented as $\mathcal{A} \bigotimes_\mu^1 \mathcal{B}$. The resulting tensor $\mathcal{C}$ is computed as

$$\mathcal{C}(i_1, \ldots, i_{\mu-1}, i_{\mu+1}, \ldots, i_d) = \sum_{k=1}^{n_\mu} \mathcal{A}(i_1, \ldots, i_{\mu-1}, k) \times \mathcal{B}(k, i_{\mu+1}, \ldots, i_d) \tag{2}$$

The inverse operation of contraction is decomposition. A tensor $\mathcal{C} \in \mathbb{R}^{n_1 \times n_2 \times n_{\mu-1} \times n_{\mu+1} \times \cdots \times n_d}$ can be decomposed into two smaller tensors $\mathcal{A}$ and $\mathcal{B}$ with respect to a partition of its indices $\{I_i\}_{i=1}^{\mu-1} | \{I_j\}_{j=\mu+1}^{d}$ [1], written as $\mathcal{C} = \mathcal{A} \bigotimes_\mu^1 \mathcal{B}$, where $\mathcal{A} \in \mathbb{R}^{n_1 \times n_2 \times \cdots \times n_\mu}$, $\mathcal{B} \in \mathbb{R}^{n_\mu \times n_{\mu+1} \times \cdots \times n_d}$, and $n_\mu = \min(\prod_{i=1}^{\mu-1} n_i, \prod_{i=\mu+1}^{d} n_i)$. Such decomposition can be done through QR or singular value decomposition (SVD).

A rank-r truncated decomposition of $\mathcal{C}$ is the operation that approximates $\mathcal{C}$ with $\mathcal{A} \bigotimes_\mu^1 \mathcal{B}$ such that the contraction dimension size $n_\mu = r$. This operation is realized through truncated SVD Hansen (1987): given a matrix M, suppose its SVD result is $M = U\Sigma V$ where $U = [u_1, u_2, \ldots, u_n]$, $V = [v_1, v_2, \ldots, v_n]^T$, and $\Sigma = \texttt{diag}(\sigma_1, \sigma_2, \ldots, \sigma_n)$ contains singular values in descending order, then its rank r truncation is $\hat{M} = U[:, :r]\Sigma[:r, :r]V[:r]$. This can be easily extended to high-order tensors when reshaping is inserted to make the conversion between matrices and tensors.

Definition 2.4 (Tensor Network, Tree Tensor Network)**.** A tensor network is an undirected graph $\mathcal{N} = (\mathcal{V}, \mathcal{E})$ where vertices $\mathcal{V}$ are tensors, and edges $\mathcal{E}$ are tuples of two node names and their shared index name. Tensor networks without cycles are called *tree tensor networks*. The tensor represented by a graph $\mathcal{N}$ is the contraction of all tensors over shared modes, denoted by $\mathcal{R}_\mathcal{N}$. The size of a tensor network is $\texttt{size}(\mathcal{N}) = \sum_{\mathcal{X} \in \mathcal{V}} \texttt{size}(\mathcal{X})$. We call edges with a dangling end *free indices*, and those without dangling ends *contracted indices*. For example, in Fig. 1, the resulting optimal network structure has four nodes, four free indices I_1, I_2, I_3, I_4 and three contracted indices r_1, r_2, r_3. The represented tensor of this network is

$$\mathcal{R}_\mathcal{N}(i, j, k, l) = \sum_{a=1}^{r_1} \sum_{b=1}^{r_2} \sum_{c=1}^{r_3} \mathcal{X}_1(i, a) \times \mathcal{X}_2(j, b) \times \mathcal{X}_3(a, b, c) \times \mathcal{X}_4(c, k, l) \tag{3}$$

Definition 2.5 (Tensor Network Structure Search)**.** A TN-SS problem is a tuple $(\mathcal{X}, \varepsilon)$, where $\mathcal{X}$ is the data tensor and ε is a prescribed error bound. The goal of the TN-SS algorithm is to solve the optimization problem

$$\arg\min_{\mathcal{N}} \ \texttt{size}(\mathcal{N}) \ \text{ s.t. } \|\mathcal{R}_\mathcal{N} - \mathcal{X}\|_F \leq \varepsilon \|\mathcal{X}\|_F \tag{4}$$

In other words, the TN-SS problem aims at finding the most compressed tensor network within a given error bound. In this work, we target arbitrary tree structures, excluding structures with cycles.

3 TN-SS via Canonical Dimension Tree Enumeration

This section details the proposed algorithm CADET, focusing on the systematic decoupling of structure search from numerical factorization. We first present the high level pipeline of the algorithm. Followed by that, we formalize the search space through the lens of dimension trees. Finally, we introduce the dimension tree scoring method, which utilizes precomputed singular values to estimate approximation errors without incurring the cost of iterative SVDs.

3.1 The High-Level Algorithm

Algorithm 1 outlines the primary stages of the CADET framework. The workflow adopts a paradigm of candidate enumeration followed by systematic assessment, utilizing a priority queue $\mathcal{C}$ to maintain the highest-quality structures identified during the search (Line 3). The algorithm iteratively traverses the search space

[1] We use $\{X_i\}_{i=a}^{b}$ to represent $\{X_a, X_{a+1}, \ldots, X_b\}$

Algorithm 1 Proposed tensor network structure search algorithm

Input Data tensor $\mathcal{X}$, error bound ε, number of selected candidate structures k_θ, and maximum number of nodes in the dimension tree S_θ

Output A tensor network $\mathcal{N}$ such that $\texttt{size}(\mathcal{N}) \leq \texttt{size}(\mathcal{X})$, and $\|\mathcal{R}_\mathcal{N} - \mathcal{X}\|_F \leq \varepsilon \|\mathcal{X}\|_F$

1: **function** CADET($\mathcal{X}, \varepsilon, k_\theta, S_\theta$)
2: $\quad\Omega \leftarrow$ PREPROCESS($\mathcal{X}, \varepsilon$) ▷ Precompute singular values for all tensor matricizations (Section 3.3.1)
3: $\quad\mathcal{C} \leftarrow \emptyset$
4: $\quad$**for** $T_\mathcal{I} \in$ ENUMDIMTREES(INDICES($\mathcal{X}$), S_θ) **do** ▷ Enumerate candidate dim trees (Section 3.2)
5: $\quad\quad c, \rho \leftarrow$ GETCOST($\Omega, \mathcal{X}, \varepsilon, T_\mathcal{I}$) ▷ Compute cost via constraint solving (Section 3.3.2)
6: $\quad\quad$add $(T_\mathcal{I}, c, \rho)$ to $\mathcal{C}$ and remove trees with large costs to maintain $|\mathcal{C}| \leq k_\theta$
7: $\quad\mathcal{N}_{\min} \leftarrow (\{\mathcal{X}\}, \emptyset)$
8: $\quad$**for** $(T_\mathcal{I}, c, \rho) \in \mathcal{C}$ **do**
9: $\quad\quad\mathcal{N}_{\min} \leftarrow \min(\mathcal{N}_{\min}, \text{DECOMPOSE}(\mathcal{X}, T_\mathcal{I}, \rho))$ ▷ Decompose $\mathcal{X}$ into $T_\mathcal{I}$ with ranks ρ (Section 3.4)
10: $\quad$**return** $\mathcal{N}_{\min}$

by generating candidate dimension trees (Lines 4–6). Within this loop, the quality of each candidate $T_\mathcal{I}$ is evaluated by calculating a cost c (Line 5), which determines the priority of the structure within $\mathcal{C}$ (Line 6). Once the top-k_θ candidate structures are established, full tensor decompositions are performed to compress the input data tensor $\mathcal{X}$ into these specific topologies, ultimately returning the structure that yields the minimum tensor network size (Lines 7–10).

There are two technical insights in this algorithm design. First, the search space is restricted to a specific subset of dimension trees to effectively exclude suboptimal and duplicate network skeletons from the enumeration process (Section 3.2). Second, CADET eliminates the requirement for tensor decompositions during the screening of candidates. By executing a one-time preprocessing of the data tensor to construct a metadata map Ω, the algorithm stores the singular values for all valid index partitions, or tensor matricizations (Line 2). Leveraging the property that singular values associated with a specific index partition are monotonically non-increasing following tensor truncation, the framework utilizes these precomputed singular values as a computationally efficient proxy to estimate candidate costs (Section 3.3).

3.2 Network Topology Exploration via Dimension Tree Enumeration

In this section, we establish a systematic framework for navigating the space of tensor network topologies. We first introduce *generalized dimension trees* (GDTs) as a formal representation of network topologies. By relaxing the exhaustive partitioning requirements of traditional dimension trees Grasedyck (2010); Falcó et al. (2021), GDTs can represent a significantly broader class of networks, including those with free indices on non-leaf nodes and multiple indices assigned to a single leaf.

To ensure search efficiency, we incorporate pruning rules within this representation to eliminate suboptimal topologies early in the process. Furthermore, since a single network topology can be mapped to multiple valid GDTs, we define a *canonical dimension tree* (CDT). This canonical form establishes a one-to-one mapping between the tree structure and the underlying topology, effectively removing redundancy during the enumeration phase.

Definition 3.1 (Generalized Dimension Trees)**.** Let $\mathcal{I} = \{I_1, \ldots, I_d\}$ be the set of free indices associated with a d-dimensional tree tensor network $\mathcal{N}$. A tree $T_\mathcal{I}$ is a generalized dimension tree of $\mathcal{I}$ if

(a) The root node is the full set $\mathcal{I}$; every other node v corresponds to a non-trivial subset of $\mathcal{I}$;

(b) For any node v, its children $\{c_1, c_2, \ldots, c_k\}$ constitute non-trivial, mutually disjoint subsets of v, such that $c_i \subset v, c_i \neq \emptyset$ for all i and $c_i \cap c_j = \emptyset$ for all $i \neq j$;

(c) For any pair of children u, v of the root, $u \cup v \neq \mathcal{I}$.

Nodes with no children are called leaf nodes. We use $\texttt{children}(T_\mathcal{I}, \mathcal{I}_s)$ to represent children nodes of $\mathcal{I}_s \in T_\mathcal{I}$.

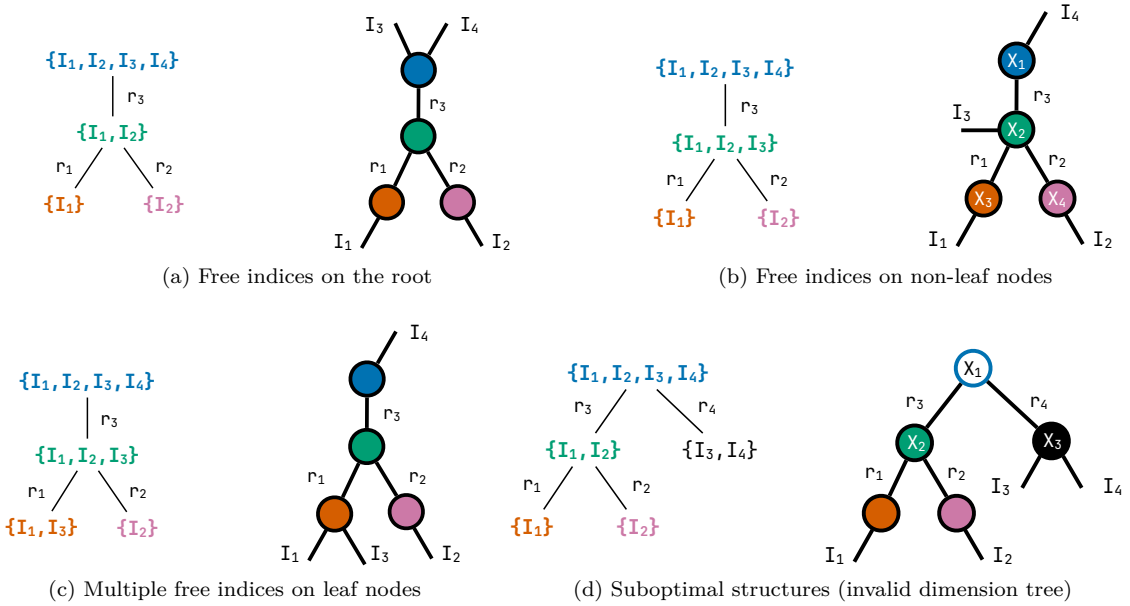

(a) Free indices on the root

(b) Free indices on non-leaf nodes

(c) Multiple free indices on leaf nodes

(d) Suboptimal structures (invalid dimension tree)

Figure 2: Examples of generalized dimension trees and their corresponding tensor network skeletons. Unfilled nodes represent structures that lead to sub-optimality, which can be merged with adjacent neighbors to reduce the total network size. Node labels in (b) and (d) are provided for ease of reference in the text.

The main differences between generalized dimension trees and traditional dimension trees are requirements (b), and (c). Requirement (b) relaxes the exhaustive partitioning of indices among children found in traditional dimension trees. Instead, it allows a node to contain indices that do not appear in any of its children; these indices are thus designated as free indices of that specific node. Requirement (c) excludes structures with suboptimal nodes.

Figure 2 illustrates the versatility of generalized dimension trees in representing diverse tensor network topologies. Unlike conventional partition trees where the union of children's indices must exhaustively cover the parent's set, this generalized framework accommodates indices at multiple hierarchical levels. As shown in Fig. 2a and Fig. 2b, free indices can be associated directly with the root and other non-leaf nodes, respectively. Furthermore, Fig. 2c demonstrates that leaf nodes may support multiple free indices simultaneously. This representation allows for the identification of suboptimal configurations; for instance, the dimension tree in Fig. 2d is invalid because it contains two nodes $\{I_1, I_2\}$ and $\{I_3, I_4\}$ that sums up to the total index set, violating the requirement (c) of dimension tree's definition. While this structure resembles a traditional Hierarchical Tucker (HT) format Grasedyck (2010), the root node $\mathcal{X}_1$ serves no purpose and only adds unnecessary parameters. Specifically, without merging, the total size of nodes $\mathcal{X}_1$, $\mathcal{X}_2$, and $\mathcal{X}_3$ is $r_3 r_4 + r_1 r_2 r_3 + r_4 n_3 n_4$. The uncolored node $\mathcal{X}_1$ can be merged with adjacent neighbors to reduce the total network size: if $r_3 < r_4$, $\mathcal{X}_1$ should be merged to the right neighbor $\mathcal{X}_3$, reducing the total size into $r_1 r_2 r_3 + r_3 n_3 n_4$; if $r_3 > r_4$, $\mathcal{X}_1$ should be merged to the right neighbor $\mathcal{X}_2$, reducing the total size into $r_1 r_2 r_4 + r_4 n_3 n_4$. Both reduced sizes are strictly lower than the unmerged sizes. To summarize, this GDT mapping ensures that the search space is both inclusive of necessary topologies and pruned of inherently inefficient skeletons.

Definition 3.2 (Generalized Dimension Tree Size)**.** Given a generalized dimension tree $T_{\mathcal{I}}$ for free indices $\mathcal{I} = \{I_1, \ldots, I_d\}$ with $n+1$ nodes $\mathcal{I}_0 = \mathcal{I}$ and $\mathcal{I}_1, \cdots, \mathcal{I}_n \subset \mathcal{I}$, and a rank assignment $\rho = \{r_i\}_{i=1}^n$ where r_i is the rank size for the edge between nodes $\mathcal{I}_i$ and its parent, and $r_0 = 1$, the size of the dimension tree $T_{\mathcal{I}}$ is recursively defined as

$$\texttt{size}\left(T_{\mathcal{I}} \mid \{r_i\}_{i=1}^n\right) = \sum_{i=0}^{n} \left(r_i \times \prod_{I \in \mathcal{I}_i \setminus \cup_c \mathcal{I}_c} \texttt{size}\left(I\right) \times \prod_c r_c + \sum_c \texttt{size}\left(T_{\mathcal{I}_c} \mid \{r_i\}_{i=1}^n\right) \right) \tag{5}$$

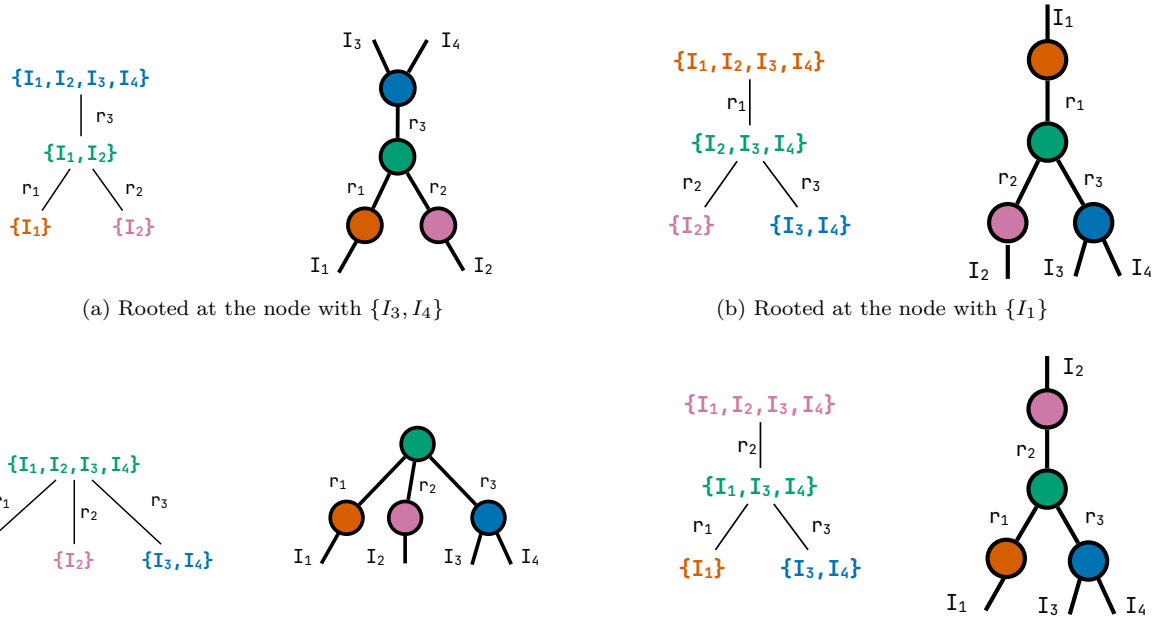

(a) Rooted at the node with $\{I_3, I_4\}$

(b) Rooted at the node with $\{I_1\}$

(c) Rooted at a node without free indices

(d) Rooted at the node with $\{I_2\}$

Figure 3: Generalized dimension trees for the same tensor network skeleton at different roots. Fig. 3a is in canonical form whereas the other three are not.

where $\mathcal{I}_c$ are the children of the node $\mathcal{I}_i$, and $T_{\mathcal{I}_c}$ are the subtrees rooted at each child node.

Intuitively, the size of a dimension tree sums up the size of all nodes inside it. As an example, consider the dimension tree in Fig. 2b with rank assignments r_1, r_2, r_3 corresponding to the edges between $(\mathcal{X}_2, \mathcal{X}_3)$, $(\mathcal{X}_2, \mathcal{X}_4)$, and $(\mathcal{X}_1, \mathcal{X}_2)$ respectively. Then the size of this dimension tree is

$$\begin{aligned}
\texttt{size}\left(T_{I_1,I_2,I_3,I_4} \mid \{r_1, r_2, r_3\}\right) = {} & \texttt{size}\left(I_4\right) \times r_3 && \text{size of node } \mathcal{X}_1 \\
& + r_3 \times \texttt{size}\left(I_3\right) \times r_1 \times r_2 && \text{size of node } \mathcal{X}_2 \\
& + r_1 \times \texttt{size}\left(I_1\right) && \text{size of node } \mathcal{X}_3 \\
& + r_2 \times \texttt{size}\left(I_2\right) && \text{size of node } \mathcal{X}_4
\end{aligned}$$

However, GDTs are not unique to a given tensor network. As illustrated in Fig. 3, a single network can yield multiple distinct dimension trees depending on the node selected as the root. This non-uniqueness introduces a significant challenge for network skeleton enumeration: the search algorithm must effectively prune redundant exploration paths to avoid the computational cost of processing equivalent structures. To eliminate this redundancy, we define a canonical dimension tree (CDT) for each tensor network and restrict the enumeration process exclusively to these canonical forms.

Definition 3.3 (Order on Index Subsets)**.** Let $\mathcal{I} = \{I_i\}_{i=1}^{d}$ be a set of indices with a lexicographical order such that $I_1 < I_2 < \cdots < I_d$. For any two subsets $\mathcal{I}_a, \mathcal{I}_b \subseteq \mathcal{I}$, we define a total order $\mathcal{I}_a < \mathcal{I}_b$ according to the following criteria:

(a) Cardinality: $\mathcal{I}_a < \mathcal{I}_b$ if $|\mathcal{I}_a| < |\mathcal{I}_b|$

(b) Lexicographical precedence: If $|\mathcal{I}_a| = |\mathcal{I}_b| = k$, and their respective sorted elements are $(a_1, \ldots, a_k)$ and $(b_1, \ldots, b_k)$, then $\mathcal{I}_a < \mathcal{I}_b$ if there exists $1 \leq j \leq k$ such that $a_j < b_j$ and $a_i = b_i$ for all $i < j$.

Under this ordering, the subsets follow the sequence $\{I_1\} < \{I_2\} < \{I_1, I_2\} < \{I_1, I_4\} < \{I_2, I_3\}$. This ordering allows us to uniquely identify a representative structure, which we define as follows:

Algorithm 2 Discover all possible canonical dimension trees for a given data tensor.

Input A set of free indices $\mathcal{I}$, and maximum number of nodes in the resulting dimension tree S_θ
Output A set of canonical dimension trees $T_\mathcal{I}$

1: **function** EnumDimTrees($\mathcal{I}, S_\theta$)
2: Initialize $T_\mathcal{I}$ with $\mathcal{I}$ being the root
3: **yield** from GrowTree($T_\mathcal{I}, S_\theta$)

4: **function** GrowTree($T_\mathcal{I}, S_\theta$)
5: **if** `size` $(T_\mathcal{I}) \geq S_\theta$ **then return**
6: **for** $\mathcal{I}_s \in T_\mathcal{I}$ **do** ▷ Enumerate all possible expansions
7: $\mathcal{I}_r \leftarrow \mathcal{I}_s \setminus \cup_{c \in \texttt{children}(T_\mathcal{I}, \mathcal{I}_s)} c$ ▷ Get remaining indices on the current node
8: **for** $\mathcal{I}_i \subset \mathcal{I}_r$ s.t. $\mathcal{I}_i \neq \emptyset$ **do** ▷ Separate a subset from remaining indices
9: **if** $\exists \mathcal{I}_j \in T_\mathcal{I}.\ \mathcal{I}_j \cup \mathcal{I}_i = \mathcal{I}$ **then continue** ▷ Well-formedness of generalized dimension trees
10: **if** $\mathcal{I} \setminus \mathcal{I}_i < \mathcal{I}_i$ **then continue** ▷ Canonical form of dimension trees
11: **if** $\exists \mathcal{I}_j \in T_\mathcal{I}.\ \mathcal{I}_j < \mathcal{I}_i$ **then continue** ▷ Enforce the expansion order to avoid duplicates
12: Add $\mathcal{I}_i$ to $T_\mathcal{I}$ as a child of $\mathcal{I}_s$ and **yield** $T_\mathcal{I}$
13: GrowTree($T_\mathcal{I}, S_\theta$)

Definition 3.4 (Canonical Dimension Trees)**.** Let $\mathcal{I}$ be the set of d free indices of a tree tensor network $\mathcal{N}$. A generalized dimension tree $T_\mathcal{I}$ is considered a canonical dimension tree of $\mathcal{N}$ if every node $\mathcal{I}_s \in T_\mathcal{I}$ satisfies either $\mathcal{I}_s = \mathcal{I}$ or $\mathcal{I}_s < \mathcal{I} \setminus \mathcal{I}_s$.

Among the four dimension trees illustrated in Fig. 3, only Fig. 3a is in canonical form. The other trees fail this criterion due to specific node violations: the nodes $\{I_2, I_3, I_4\}$ in Fig. 3b, $\{I_3, I_4\}$ in Fig. 3c, and $\{I_1, I_3, I_4\}$ in Fig. 3d all violate the canonical condition because their respective complement sets are smaller under the defined order.

3.2.1 Dimension Tree Enumeration (Procedure EnumDimTrees)

The generation of CDTs is formalized in Algorithm 2. The algorithm takes a set of free indices $\mathcal{I}$ and a parameter S_θ to control the size of output dimension trees. At a high level, the procedure initializes a tree with a single root node $\mathcal{I}$ (Line 2) in accordance with dimension tree's definition rule Item (a), and subsequently expands the structure by recursively inserting child nodes (Line 3).

The core logic resides within the GrowTree function, which employs an iterator-style approach to yield valid canonical trees. GrowTree first verifies the current tree size against the limit S_θ (Line 5). If capacity remains, the algorithm iterates through all existing nodes in the tree (Line 6) to identify potential expansion points. For a selected node, the algorithm identifies the set of indices $\mathcal{I}_r$ not yet partitioned (Line 7) and evaluates all possible non-empty subsets $\mathcal{I}_i \subset \mathcal{I}_r$ to create new child nodes (Line 8). To ensure efficiency and uniqueness, the algorithm applies three critical pruning filters:

(1) **Well-Formedness of Dimension Trees:** A new node $\mathcal{I}_i$ is discarded if, when combined with an existing sibling node $\mathcal{I}_j$, it fully partitions the index set $\mathcal{I}$. This prevents the formation of invalid trees that violate the rule Item (c) in the definition of dimension trees (Line 9).

(2) **Canonical Form of Dimension Trees:** The algorithm enforces that the enumerated trees are canonical. If the complement set $\mathcal{I} \setminus \mathcal{I}_i$ is smaller than $\mathcal{I}$ according to our defined set order, the node is skipped to ensure only the canonical form is explored (Line 10).

(3) **Insertion Order:** To prevent isomorphic trees arising from different insertion sequences (e.g., adding $\{I_1\}$ then $\{I_2\}$ versus vice-versa), we enforce a strict descending order for node introduction (Line 11). A new node is only added if it is smaller than previously added nodes in the current tree.

Once a candidate node $\mathcal{I}_i$ passes these checks, it is integrated into the tree and yielded as a valid canonical structure (Line 12). The process then continues recursively to explore deeper expansions (Line 13).

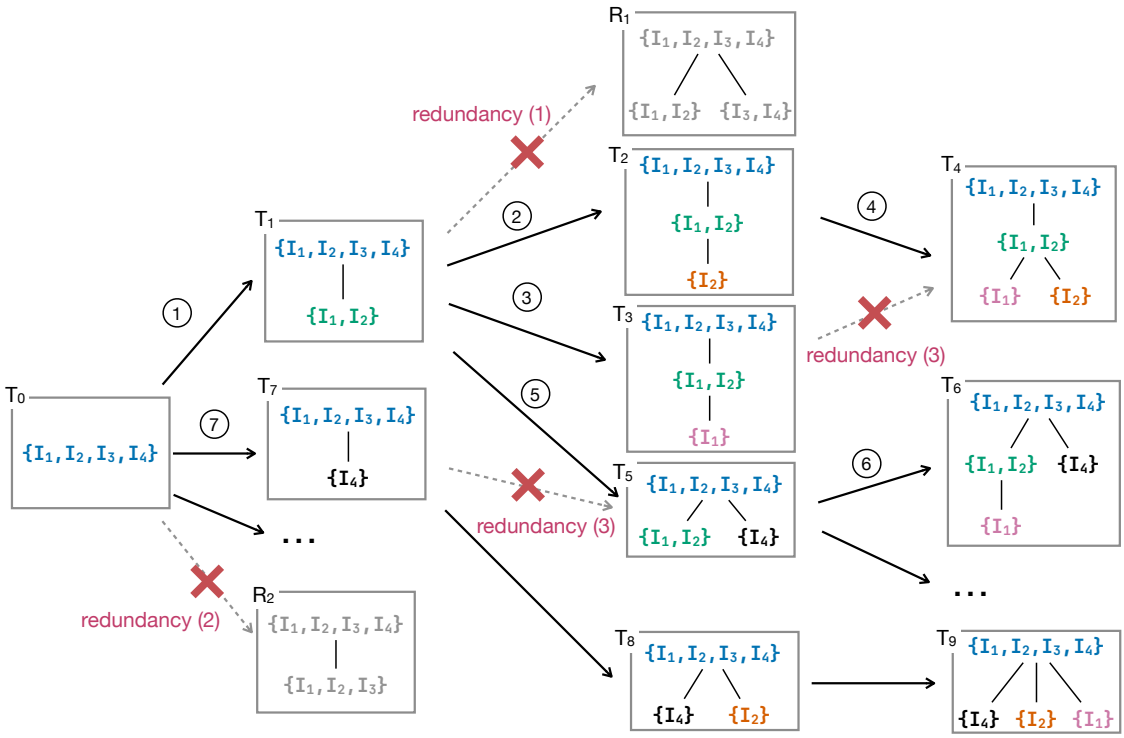

Figure 4: Enumeration of canonical dimension trees. Gray dashed edges and trees are redundant redundant enumeration paths and trees respectively, which are excluded from the search process. Three kinds of redundancy are pruned: (1) invalid dimension trees R_1 where the two sibling nodes $\{I_1, I_2\}$ and $\{I_3, I_4\}$ form a full partition of the indices; (2) non-canonical dimension trees R_2 where the node $\{I_1, I_2, I_3\}$ has a shorter complement node $\{I_4\}$, and therefore $\{I_1, I_2, I_3\}$ should never appear in a canonical dimension tree; (3) duplicate canonical dimension trees resulted from multiple enumeration paths (T_3 to T_4, T_7 to T_5). Redundancy (1) and (2) are ruled out by the definition of canonical dimension trees, while redundancy (3) is excluded by enforcing the order when adding nodes.

Figure 4 illustrates this enumeration process for a four-dimensional tensor. Starting from the single node tree T_0, the algorithm introduces child nodes such as $\{I_1, I_2\}$ (step ①), $\{I_4\}$ (step ⑦), etc. to expand the structure. Among them, the transition from T_0 to R_2 is excluded because R_2 contains the node $\{I_1, I_2, I_3\}$, violating the canonical rule of CDTs as its complement set $\{I_4\}$ is smaller in our defined order. Focusing on the valid path in step ①, the algorithm introduces the child $\{I_1, I_2\}$. From this state, the tree can grow by attaching $\{I_2\}$ (step ②) or $\{I_1\}$ (step ③) to the leaf $\{I_1, I_2\}$, or by adding a sibling node $\{I_4\}$ to the root (step ⑤). Notably, the algorithm prohibits attaching $\{I_3, I_4\}$ to the root (tree R_1) as it would violate the well-formedness rule of GDTs. Furthermore, while steps ② and ③ could eventually converge on the same structure T_4, only the path through step ④ is permitted; the transition from T_3 to T_4 is pruned by the insertion order constraint because $\{I_1\} < \{I_2\}$.

3.3 Fast Scoring Via Constraint Solving

The CDTs generated via enumeration define an expansive search space of tensor network skeletons. While these structures establish the node connectivity (topology), the associated edge weights, specifically the rank assignments for each bond, remain undetermined. A naïve approach would involve executing a full tensor decomposition for every candidate tree $T_{\mathcal{I}}$ to evaluate its performance. However, such a strategy is computationally prohibitive for large data tensors, as the cost of decomposition scales poorly regardless of the specific algorithm employed.

Algorithm 3 Precompute singular values for all matricizations of a given data tensor.

Input A set of free indices $\mathcal{I}$
Output Mapping Ω from index subsets to singular values

1: **function** PREPROCESS($\mathcal{X}$)
2: $\quad\mathcal{I} \leftarrow$ INDICES($\mathcal{X}$)
3: $\quad\Omega \leftarrow \emptyset$
4: $\quad$**for** $s = 1, 2, \ldots, \lfloor \frac{\texttt{len}(\mathcal{I})}{2} \rfloor$ **do** ▷ Enumerate all possible index subsets
5: $\quad\quad$**for** $\mathcal{I}_s \in$ SUBSETSOF($\mathcal{I}, s$) **do**
6: $\quad\quad\quad U; \Sigma; V \leftarrow \text{SVD}(\mathcal{X}^{(\mathcal{I}_s)})$
7: $\quad\quad\quad\Omega[\mathcal{I}_s] \leftarrow \texttt{diag}(\Sigma)$ ▷ Store the singular values for the unfolding at $\mathcal{I}_s$
8: $\quad$**return** Ω

To bypass this bottleneck, we propose a constraint-solving technique designed to rapidly screen candidate structures and figure out the near-optimal rank assignment at the same time. This method identifies rank configurations with the highest compression potential, significantly reducing the number of full-scale decompositions required. The fundamental insight of this approach is that the singular value spectra of the original data tensor $\mathcal{X}$ can serve as a rigorous upper bound (over-approximation) for the singular values encountered during the actual hierarchical decomposition process.

In the following sections, we detail the mechanics of this scoring framework. We first describe the one-time singular value precomputation phase (Line 2 of Algorithm 1), which populates the metadata map Ω. We then demonstrate how these precomputed singular values are utilized in a fast cost computation routine (Line 5) to evaluate candidate skeletons without the need for intermediate tensor factorizations.

3.3.1 Pre-computation of Singular Values (Procedure Preprocess)

At the initialization of CADET (Line 2), we construct a metadata map Ω to store the singular values for all possible matricizations of the input data tensor. As detailed in Algorithm 3, the tensor $\mathcal{X}$ is unfolded along every subset of its free indices $\mathcal{I}$ (Line 4). For each matricization $\mathcal{X}^{(\mathcal{I}_s)}$, we perform SVD to extract the associated singular values (Line 6). These information are indexed by their corresponding index sets $\mathcal{I}_s$ and archived in Ω (Line 7). While this preprocessing is the most computationally expensive phase of the algorithm with a complexity that grows exponentially with the number of dimensions, it is a one-time cost that serves as a high-speed look-up table for the assessment phase. Since the algorithm bypasses online decompositions during the evaluation of thousands of candidate skeletons, it remains highly efficient. For very high-dimensional tensors, this costly preprocessing step can be embedded within a hierarchical search framework to reduce the high computation complexity Guo et al. (2026).

3.3.2 Constraint-Based Rank Optimization and Assessment (Procedure GetCost)

While CADET can exhaustively enumerate a vast library of dimension trees, each representing a distinct tensor network skeleton, it is computationally prohibitive to perform explicit tensor decompositions to identify the optimal rank assignment for every candidate. Even with fixed ranks, the cost of iterative factorizations remains the primary bottleneck in the search process (Section 5.3). To overcome this, we treat rank assignment not as a search variable, but as a constrained optimization problem solved analytically for each dimension tree.

Given a data tensor $\mathcal{X}$, an error bound ε, and a dimension tree $T_{\mathcal{I}}$ with $n+1$ nodes where $\mathcal{I}_0 = \mathcal{I}$ and $\mathcal{I}_1, \mathcal{I}_2, \ldots, \mathcal{I}_n \subset \mathcal{I}$, we formulate the task of GETCOST as finding the rank assignment $\rho = \{r_s\}_{s=1}^n$ that minimizes the dimension tree size while satisfying the error budget. Leveraging the precomputed singular value in Ω, we model this as the following integer programming problem:

$$\min_{r_1, r_2, \ldots, r_n} \texttt{size}\left(T_{\mathcal{I}} \mid \{r_s\}_{s=1}^n\right) \quad \text{s.t.} \quad \sum_{s=1}^{n} \sum_{i > r_s} \Omega^2[\mathcal{I}_s, i] \leq \left(\varepsilon \|\mathcal{X}\|_F\right)^2 \tag{6}$$

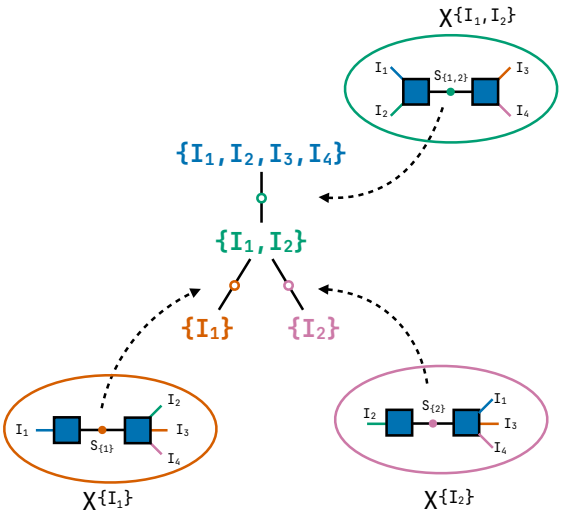

Figure 5: Approximation of singular values during decomposition using those of the input data tensor. Big circles denote the pre-computed SVD results over different matricizations of the input tensor. Solid small dots represent singular values for the data tensor, and unfilled small circles represent the location of what singular values we are approximating.

In this formulation, each r_s is an integer variable for the edge rank between node $\mathcal{I}_s$ and its parent, and $\Omega[\mathcal{I}_s, i]$ represents the i^{th} largest singular value for the $\mathcal{I}_s$ unfolding of data tensor $\mathcal{X}$. The constraint ensures that the cumulative truncation error, which is equal to the sum of discarded singular values across all n edges, remains within the threshold ε. Once solved, the resulting rank assignment ρ is recorded and the corresponding dimension tree size serve as the cost metric used to rank the trees.

As illustrated in Fig. 5, this approach approximate hierarchical tensor decompositions described in a dimension tree with a sequence of independent tensor decompositions applied to the original data tensor. For a dimension tree defined by the nested index sets $\{I_1, I_2, I_3, I_4\}$, $\{I_1, I_2\}$, $\{I_2\}$, and $\{I_1\}$, we approximate the singular values at each edge using the precomputed $\Omega[\{I_1, I_2\}]$, $\Omega[\{I_2\}]$, and $\Omega[\{I_1\}]$. This methodology is theorectically supported by the following property:

Theorem 3.5 (Singular Value Upper Bound)**.** *Let $\mathcal{X} \in \mathbb{R}^{n_1 \times \cdots \times n_d}$ be a d-dimensional tensor, compressing $\mathcal{X}$ into a structure described by a dimension tree $T_{\mathcal{I}}$ of $n+1$ nodes $\mathcal{I}, \mathcal{I}_1, \mathcal{I}_2, \ldots, \mathcal{I}_n$ produces the structure $\mathcal{N}$, then for every $1 \leq i, s \leq n$, we have $\sigma_j\left(\mathcal{R}_{\mathcal{N}_i}{}^{(\mathcal{I}_s)}\right) \leq \sigma_j\left(\mathcal{X}^{(\mathcal{I}_s)}\right)$ where $\sigma_j(A)$ is the j^{th} largest singular value of the matrix A, and $\mathcal{N}_i$ is the network obtained after the first i tensor decompositions specified by $T_{\mathcal{I}}$.*

Proof. By the definition of dimension trees, for every pair $1 \leq s < t \leq n$, there could only be three relations between $\mathcal{I}_s$ and $\mathcal{I}_t$: $\mathcal{I}_s \subset \mathcal{I}_t$, $\mathcal{I}_t \subset \mathcal{I}_s$, or $\mathcal{I}_s \cap \mathcal{I}_t = \emptyset$.

Suppose the network obtained after the k^{th} tensor decomposition is denoted as $\mathcal{N}_k$. The network obtained after performing the tensor decomposition on $\mathcal{N}_k$ along index set $\mathcal{I}_k$ is $\mathcal{N}_{k+1}$. Performing the split defined above is equivalent to performing a truncated SVD on $\mathcal{R}_{\mathcal{N}_k}{}^{(\mathcal{I}_k)}$. Formally, we can say that if $\mathcal{R}_{\mathcal{N}_k}{}^{(\mathcal{I}_k)} = U\Sigma V$, then $\mathcal{R}_{\mathcal{N}_{k+1}}{}^{(\mathcal{I}_k)} = \widetilde{U}\widetilde{\Sigma}\widetilde{V}$, where $\widetilde{U}$, $\widetilde{\Sigma}$, and $\widetilde{V}$ are truncated matrices of U, Σ, and V. Consequently, using Theorem A.5, we have that, for $\mathcal{I}_t \subset \{I_1, \ldots, I_d\}$ such that $\mathcal{I}_t \subseteq \mathcal{I}_s, \mathcal{I}_s \subseteq \mathcal{I}_t$, or $\mathcal{I}_s \cap \mathcal{I}_t = \emptyset$, $\sigma_i\left(\mathcal{R}_{\mathcal{N}_{k+1}}\right) \leq \sigma_i\left(\mathcal{R}_{\mathcal{N}_k}\right)$ for all possible i and k.

From the above result, we can conclude that $\sigma_i\left(\mathcal{R}_{\mathcal{N}_k}{}^{(\mathcal{I}_t)}\right) \leq \sigma_i\left(\mathcal{R}_{\mathcal{N}_0}{}^{(\mathcal{I}_t)}\right) = \sigma_i\left(\mathcal{X}^{(\mathcal{I}_t)}\right)$ for all valid choices of $\mathcal{I}_t$ and all possible values of i and k. □

Theorem 3.5 allows us to use the singular values of the original data as a rigorous over-approximation for any candidate dimension tree. While this may lead to a conservative estimate of the truncation error, we find that this upper bound is an exceptionally effective proxy for ranking. By solving for this bound, CADET

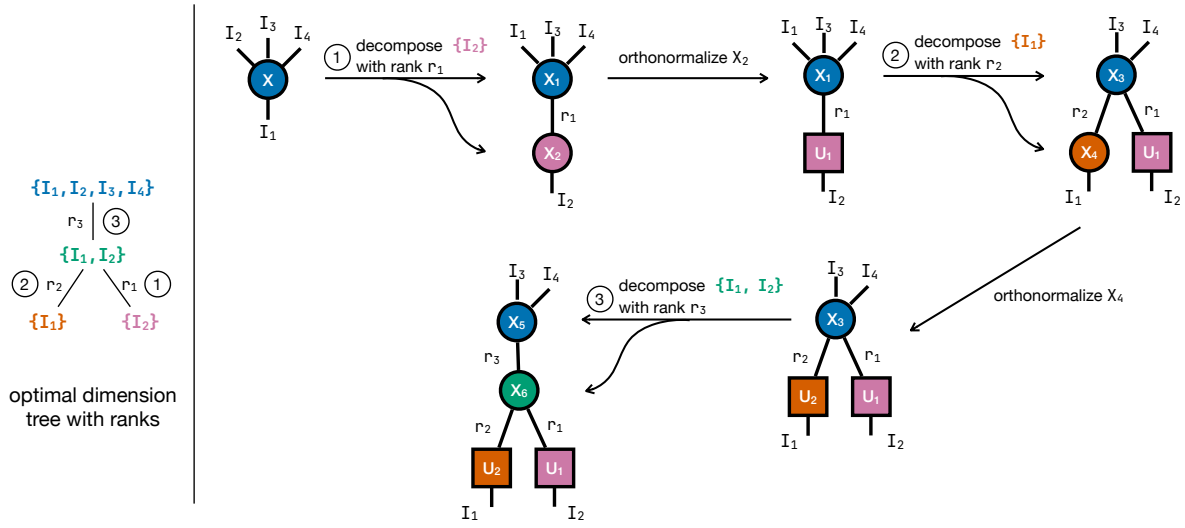

Figure 6: Decompose a data tensor into the format described by a generalized dimension tree. (left) A generalized dimension tree with rank assignments. (right) Step-by-step transformation from a data tensor to the tensor network represented by the dimension tree on the left. The tensor decomposition and network orthonormalization interleaves to ensure truncation error correctly propagates from individual nodes to the entire network. Square nodes stand for orthogonal nodes.

identifies high-performance dimension trees without the prohibitive overhead of live tensor decompositions during the search phase.

3.4 Tensor Decomposition From Dimension Trees (Procedure Decompose)

The final step of CADET is involves the physical transformation of the data tensor into the tensor network structures dictated by the highest-ranked dimension trees (Lines 7–10 of Algorithm 1). Unlike the assessment phase, which operates on Ω, the DECOMPOSE procedure executes a sequence of tensor decompositions, using the determined rank assignments ρ as the bond dimensions.

The hierarchical structure of the generalized dimension tree $T_{\mathcal{I}}$ serves as a blueprint for this process. Each non-root node in $T_{\mathcal{I}}$ prescribes a specific bipartition that incrementally shapes the network topology. As illustrated in Fig. 6, the process begins at a leaf representing an index set $\{I_2\}$, and isolates these indices via a r_1 truncated SVD along the bipartition $\{I_2\}|\mathcal{I} \setminus \{I_2\}$, splitting the data tensor into two factors (step ①).

When moving to the leaf $\{I_1\}$, the algorithm identifies $\mathcal{X}_1$ as the target node. To ensure the subsequent steps correctly compute the singular values, the algorithm must shift the orthogonality center between splits. Standard tensor network theory dictates that a local SVD only yields the true, global singular values of a bipartition if the operating node concentrates the system's full norm White (1992; 1993); Evenbly (2022). Therefore, the previously created factor $\mathcal{X}_2$ is orthonormalized into the isometry $\mathcal{U}_1$, pushing the global norm into $\mathcal{X}_1$. Then, the second decomposition performed to separate index I_1 (step ②).

For the non-leaf node $\{I_1, I_2\}$, the algorithm identifies the node in the current network that serves as the lowest common ancestor to both the I_1 and I_2 branches. In our example, this common ancestor is $\mathcal{X}_3$. After centering the orthogonality at $\mathcal{X}_3$ by orthonormalizing surrounding tensors, a further decomposition splits it into $\mathcal{X}_5$ and $\mathcal{X}_6$ to achieve the desired index partition (step ③).

Following the completion of the hierarchical decomposition, the resulting network approximates the original data $\mathcal{X}$ within the relative error bound ε. However, as established by Theorem 3.5, the singular values used during the constraint-solving phase are rigorous over-approximations derived from the original tensor. This implies that the solved ranks ρ may be more conservative than strictly necessary. To recover these potential gains, we apply a rounding procedure, an extension of the TT-rounding algorithm Oseledets (2011) adapted

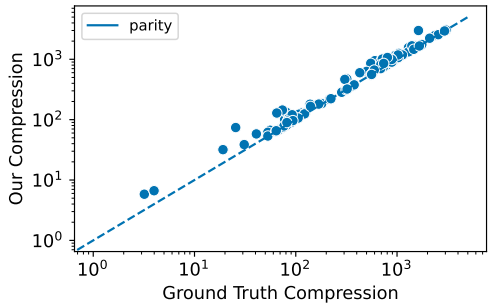

Figure 7: Comparison of compression ratios for random generated data. Ground truth compression is the compression ratio of the structure used to generate synthetic data.

for tree structures to exhaust the remaining error budget. Notably, we employ the solved ranks ρ in the final decomposition rather than adopting an even error distribution across decomposition stages as common in TT or HT decomposition. In practice, we observe that this strategy yields improved compression ratios by utilizing the specific rank assignment identified by the solver.

4 Complexity Analysis

Given a tensor of d dimensions and each dimension has size n, the preprocessing phase runs the SVD for all possible index partitions, which takes time $\mathcal{O}\left(n^{1.5d}2^d\right)$. Then, the algorithm enumerates all dimension trees with at most S_θ nodes. The total number of dimension trees is $\mathcal{O}\left(2^{S_\theta d}\right)$. For each dimension tree, a constraint solving is run to compute the rank assignment, each taking time $\mathcal{O}\left(S_\theta^{2.5}2^{S_\theta}\right)$. Lastly, we compress the data tensor for the best dimension tree, which involves at most S_θ truncated SVDs. Therefore, the total complexity is $\mathcal{O}\left(n^{1.5d}(S_\theta + 2^d) + S_\theta^{2.5}2^{S_\theta + S_\theta d}\right)$. In practice, when $d \leq 6$ and $S_\theta \leq 6$, the algorithm produces good compression ratios. We leave the support of higher-dimensional data as future work.

5 Evaluation

In this section, we present empirical evaluation results, which aim to answer the following questions:

- **(RQ1)** Can CADET discover well-compressed structures for synthetic and real data?
- **(RQ2)** How does the performance of CADET compare to prior work?
- **(RQ3)** How useful are CDT-based enumeration and constraint-based ranking in the search?
- **(RQ4)** Can the structures discovered by CADET generalizable to unseen data?

General Experiment Setup We run all the following experiments on a laptop with the Apple M3 Max CPU and 128 GB memory. In the experiments, we collect the running time and the compression ratio, which is defined as $\texttt{size}(\mathcal{X})/\texttt{size}(\mathcal{R}_\mathcal{N}) = \texttt{size}(\mathcal{X})/\sum_{v\in\mathcal{V}}\texttt{size}(v)$. We choose the top k_θ structure for actual decomposition from all enumerated candidates.

5.1 RQ1: Compression Performance of Cadet on Synthetic and Real Data

5.1.1 Performance on Synthetic Data

Experiment Setup We evaluate our algorithm on synthetic data by generating random tensors contracted from random tree structures. This provides a basic test that our algorithm can identify structures with compression ratios equal to or better than the generation structure. Following prior work Zheng et al. (2024), we generate order-4 tensors with dimensions $16 \times 18 \times 20 \times 22$ and order-5 tensors with dimensions $14 \times 16 \times 18 \times 20 \times 22$. Internal ranks are randomly sampled between 2 and 5. For each shape, we sample 50 structures with random tensor values, and contract them into data tensors.

Table 1: Average compression ratio (CR), search time in seconds, and reconstruction error (RE) of CADET on real datasets for error bounds $\varepsilon = 0.1$ and $\varepsilon = 0.01$.

	$\varepsilon = 0.1$			$\varepsilon = 0.01$		
Data	CR	Time (s)	RE	CR	Time (s)	RE
Light field ($40 \times 60 \times 3 \times 9 \times 9$)	68.34	16.07	0.098	7.04	10.17	0.010
BigEarthNet ($30 \times 12 \times 120 \times 120$)	155.71	4.67	0.099	2.69	8.07	0.010
BigEarthNet ($5 \times 20 \times 30 \times 12 \times 120 \times 120$)	151.73	4914.70	0.099	3.07	5074.46	0.010
PDEBench ($10 \times 5 \times 21 \times 64 \times 64 \times 64$)	38.75	2222.05	0.099	1.81	2660.13	0.010

Result Analysis Fig. 7 compares the compression ratios of generation structures and those discovered by CADET. The results indicate that CADET achieves compression ratios that are equal to or greater than that of generation structures, for every data point. In other words, CADET identifies improved structures when the generation structure is not optimal.

5.1.2 Performance on Real Data

Experiment Setup To evaluate the performance of CADET on real-world data, we employ three datasets: light fields Zheng et al. (2024), BigEarthNet Sumbul et al. (2019), and PDEBench Takamoto et al. (2022a;b). For the light field data, we use the bunny data with dimensions $40 \times 60 \times 3 \times 9 \times 9$, following prior work Zheng et al. (2024). The BigEarthNet data is used to create tensors with dimensions $30 \times 12 \times 120 \times 120$ and $5 \times 20 \times 30 \times 12 \times 120 \times 120$ by randomly sampling and stacking 30 and 3000 data points respectively. For the PDEBench data, we sample 10 data points from the 3D compressible Navier-Stokes problem to create tensors of dimensions $10 \times 5 \times 21 \times 64 \times 64 \times 64$.

Result Analysis We collect average compression ratios, search time in seconds, and reconstruction errors for each dataset in Table 1. The results demonstrate that CADET achieves significant compression across diverse real-world datasets while strictly adhering to the prescribed error bounds. For an error tolerance of $\varepsilon = 0.1$, the algorithm yields high compression ratios, notably above 150 for the BigEarthNet datasets. As the error bound tightens to $\varepsilon = 0.01$, the compression naturally decreases, ranging from 1.81 to 7.04. The search time increases with the size and order of the data. For small data tensors with low dimensionality, the search time is usually below 20 second. For large data tensors, the search time rises up to around 5000 second. The stable reconstruction errors across all benchmarks confirm that precomputed singular values provides an upper bound for real singular values: CADET uses precomputed singular values to search for rank assignments, and none of the numerical experiments witness the exceeding of the prescribed error bounds.

5.2 RQ2: Compression Performance Comparison Between Cadet and Existing Tools

Experiment Setup We compare our method in terms of search time and compression ratio against tensor trains (TT), binary hierarchical tuckers (HT), and three baselines: (1) GreedyTN Hashemizadeh et al. (2020): a greedy algorithm that gradually increases internal ranks; (2) TnALE Li et al. (2023): a sampling-based method that reduces sample sizes by local search; (3) SVDinsTN Zheng et al. (2024): an optimization-based approach that integrates rank and topology search. For our algorithm, we search dimension trees of up to 6 nodes and pick the top one for the tensor decomposition. The timeout limit is 3 hours.

Result Analysis The results are shown in Fig. 8. Compared to TT and HT, our algorithm finds more compressed structures, albeit requiring roughly an order of magnitude more time across all datasets. This is expected, as our approach explores general tree structures and allows reordering free indices, whereas TT and HT are limited to special cases within our broader search space.

In comparison to prior work, our method not only achieves comparable or superior compression ratios, especially on large tensors, but is also at least 10× faster than baselines. While TnALE occasionally discovers structures with higher compression ratios by finding cyclic structures, its dependence on a large sample

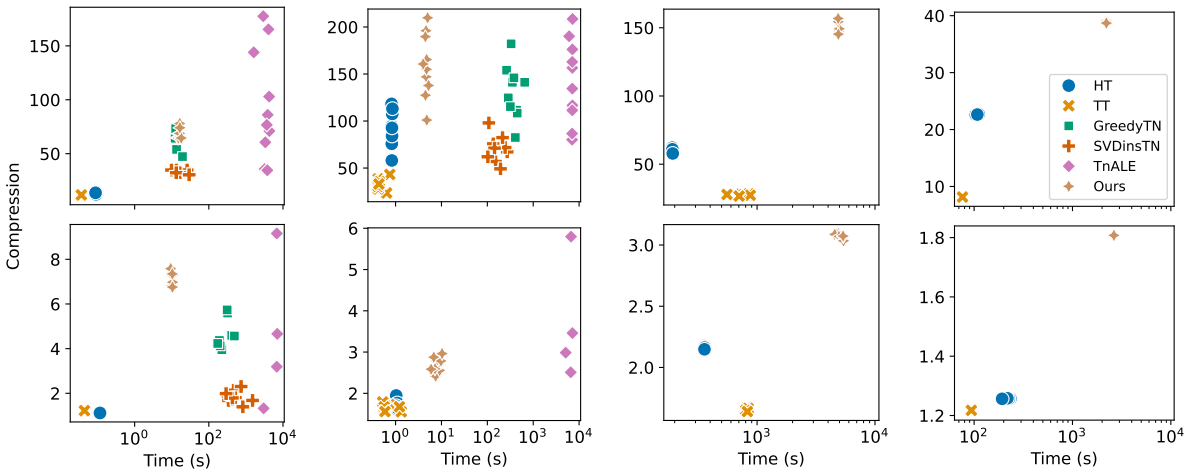

Figure 8: Comparison of compression ratio vs time on real datasets. The datasets from left to right are light field data ($40 \times 60 \times 3 \times 9 \times 9$), BigEarthNet ($30 \times 12 \times 120 \times 120$), BigEarthNet ($5 \times 20 \times 30 \times 12 \times 120 \times 120$), and PDEBench ($10 \times 5 \times 21 \times 64 \times 64 \times 64$). The two rows corresponds to error bounds of 0.1 and 0.01 respectively.

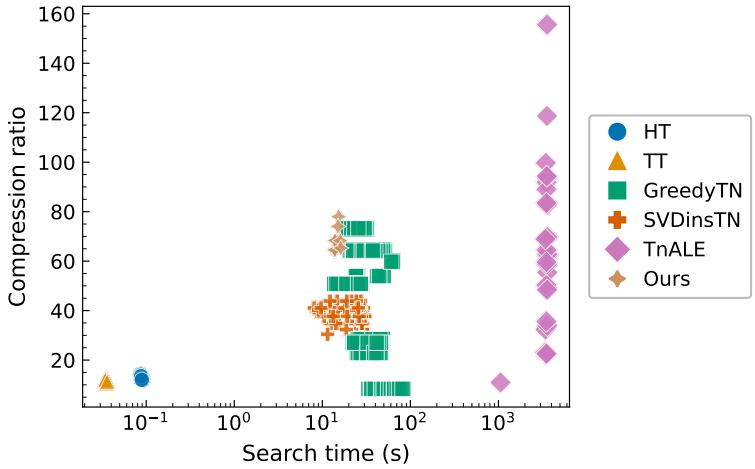

Figure 9: Compression Ratio vs. Runtime on Light Field Data ($40 \times 60 \times 3 \times 9 \times 9$) with $\varepsilon = 0.1$ and a timeout limit 1 hour. Each data point of the baselines represents the structure search result for a data tensor with a specific hyperparameter configuration. The proposed method (Ours) achieves competitive compression while remaining orders of magnitude faster than high-performance baselines like TnALE.

size leads to significant slowdowns across tests. Moreover, TnALE often fails to converge to the desired error bound within the timeout, and encounters out-of-memory issues with large tensors. TNGreedy and SVDinsTN exhibit performance similar to ours on smaller tensors and larger error bounds, but neither scales well as tensor size increases. They do not produce results within the 3-hour timeout for BigEarthNet data with $\varepsilon = 0.01$ or other larger tensors with either error bound.

To verify that the performance gains of CADET are consistent across different baseline parameterizations, we conducted an extensive parameter sweep on the light field dataset with $\varepsilon = 0.1$ and timeout limit of 1 hour. We tested a broad range of configurations for each baseline: rank boundaries from $[10, 15, 20]$ for TnALE; optimization steps from $[100, 200, 300]$, rank increments from $[1, 2, 4]$, and ALS iterations from $[100, 150, 200]$ for GreedyTN; and the regularization parameters $\gamma \in [0.05, 0.1, 0.5]$, $\mu \in [0.1, 0.5, 1.0]$, and $\rho \in [10^{-4}, 10^{-5}, 10^{-6}]$ for SVDinsTN. These parameter choices are centered around the manually tuned

Table 2: Comparison of compression ratio (CR) and runtime on Light field data $60 \times 40 \times 3 \times 9 \times 9$, and BigEarthNet $30 \times 12 \times 120 \times 120$ data across different variants of our algorithm. The variants differ based on the dimension tree enumeration method (canonical or non-canonical) and the rank search method (constraint-based or equal error distribution). Canonical + Constraint is ours. Results are shown for error bounds $\varepsilon = 0.1$ and $\varepsilon = 0.01$.

Dataset	Variant		$\varepsilon = 0.1$		$\varepsilon = 0.01$	
	Enum	Rank	CR	Time (s)	CR	Time (s)
Light field $40 \times 60 \times 3 \times 9 \times 9$	Canonical	Constraint	68.34	**16.07**	7.03	**3.62**
	Non-canonical	Constraint	68.34	4069.6	7.03	1635.2
	Canonical	Equal	69.18	28.73	7.03	44.32
BigEarthNet $30 \times 12 \times 120 \times 120$	Canonical	Constraint	155.71	**4.67**	2.69	**8.07**
	Non-Caonical	Constraint	154.64	1248.06	2.66	419.65
	Canonical	Equal	147.51	15.04	2.62	68.97

Table 3: Performance of network search on the training batch, optimal discovered network on the test batches, and hierarchical Tuckers (HT) on the test batch with respect to compression ratios and time.

	BigEarthNet		PDEBench	
	CR	Time (s)	CR	Time (s)
Train	157.12	4591.64	38.75	2141.85
Test	148.98	109.61	38.58	115.38
HT	60.71	190.98	22.65	95.21

settings used in the previous experiment. Due to the significant runtime of the baselines, this exhaustive sweep was restricted to the light field data as a representative benchmark.

As shown in Fig. 9, the resulting performance trends mirror our previous evaluation in Fig. 8 (top left). CADET provides a superior balance of efficiency and compression performance, identifying high-quality structures with small search overhead. While TnALE can reach higher absolute compression ratios, largely due to its support for cyclic topologies, it requires orders of magnitude more search time and frequently hits the one-hour timeout. GreedyTN exhibits significant performance variance across different parameter settings and tensors, but no configuration reaches the compression performance of our method. SVDinsTN is more stable, but it frequently converges to suboptimal structures or fails to satisfy the error bound. In contrast, our approach CADET identifies high-quality tensor network structures without the need for the extensive hyperparameter tuning that limits the practical utility of existing methods.

These results confirm that our method outperforms baselines in terms of search time and compression ratio. Our method of deferring decomposition until the search space is narrowed down effectively reduces the search time. However, the lack of support for cycles limits our performance on compression ratio in some cases, and we plan to address this in future work.

5.3 RQ3: Ablation Studies

5.3.1 Dimension Tree Enumeration w/ vs w/o Canonicalization

We evaluate the effectiveness of canonical dimension tree enumeration by comparing its performance to general tree enumeration (removing the three checks on lines 9–11 of Algorithm 2). We set the maximum number of nodes in dimension trees to 6. We compare compression ratios and running time of the two settings on light field data with dimensions $40 \times 60 \times 3 \times 9 \times 9$, and BigEarthNet data with dimensions $30 \times 12 \times 120 \times 120$. Ablation experiments on larger tensors did not produce results within 12 hours and are therefore omitted. Table 2 shows that both methods achieve similar compression ratios, but canonical

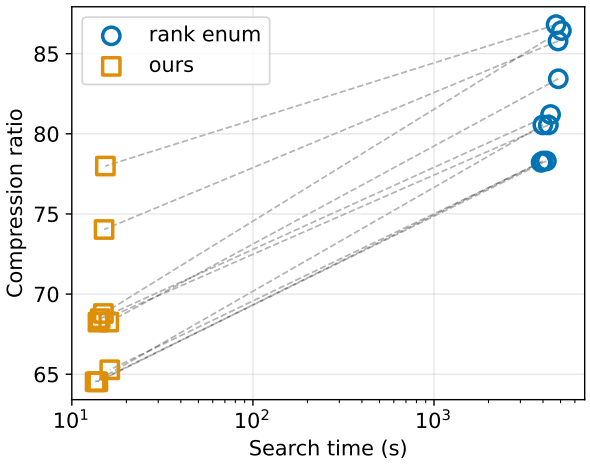

Figure 10: Performance comparison between constraint-based and rank-enumeration-based scoring for light field data. The proposed constraint-based method reduces search time by approximately two orders of magnitude at the cost of a moderate reduction in compression ratio (CR), which remains within 80-85% of the rank-enumeration method. Dotted lines indicate corresponding data points between two methods.

dimension tree enumeration significantly accelerates the search process because allowing canonical checks results in only 63 CDTs whereas removing canonical checks leads to 35727 trees.

5.3.2 w/ vs w/o Constraint-Based Rank Search

To evaluate the effectiveness of constraint-based rank search, we compare it against a variants that enumerates all possible rank assignments for a tree. Figure 10 presents the changes of compression ratios and search time for the 10 light field data tensors at $\varepsilon = 0.1$. It shows that our proposed method reduces the search time by approximately two orders of magnitude while maintaining high compression ratios, typically reaching 80–90% of the values found by the exhaustive rank-enumeration method.

However, it is unaffordable to run exhaustive rank enumeration on light field data with $\varepsilon = 0.01$ or BigEarthNet data with either error tolerance, we develop a cheaper variant that distributes the error budget equally between steps, which is the strategy adopted by HT and TT. The results in Table 2 demonstrate that this variant not only achieves a lower compression ratio but is also slower than the constraint-solving approach. Our constraint-based rank search method avoids performing actual data fitting for each dimension tree by using a constraint solver, which reduces computation time, especially for small error bounds.

5.4 RQ4: Generalization Analysis

Experiment Setup We conduct a generalization test to evaluate if the structure discovered by our algorithm generalizes to unseen data. To begin, each dataset is divided into equal-sized batches. The first batch serves as the training batch, where both topology and rank search are performed using the proposed algorithm. For subsequent test batches, we apply the topology from the training batch, and run the constraint-based rank search to assess generalization. In the BigEarthNet dataset, data is divided into 89 batches of tensors with shape $5 \times 20 \times 30 \times 12 \times 120 \times 120$, each containing 3000 samples. In the PDEBench dataset, the data is divided into 60 batches of 10 samples each, producing tensors of shape $10 \times 5 \times 21 \times 64 \times 64 \times 64$. The error bound used for this experiment is $\varepsilon = 0.1$.

Result Analysis Table 3 presents the compression ratios and running time for the training batch and the averages of test batches. The results show that the compression ratios of test batches are close to that of the training batch, which proves that the discovered topology generalizes well to unseen data. Particularly, although the training batch requires thousands of seconds to find the optimal structure, it takes only about

110 seconds on average to perform the decomposition for each test batch. This result reinforces the feasibility of running the training batch once to determine the optimal topology and reusing it for subsequent batches, which significantly reduces the overall computation time.

6 Conclusion and future work

In this work, we introduced a framework for tensor network structure search based on generalized dimension trees. By representing potential architectures as hierarchical index partitions, we successfully decouple topology enumeration from rank optimization, a strategy that significantly reduces the complexity of the search space. Our methodology replaces the traditional, computationally expensive candidate assessment methods with an efficient constraint-solving mechanism. By precomputing a metadata map of singular values, we are able to analytically solve for optimal ranks and evaluate candidate quality without performing live tensor decompositions for every structure in the search space.

Our empirical results on both synthetic and real-world datasets demonstrate that the proposed approach consistently discovers well-compressed structures, achieves higher compression ratios than existing baselines, and scales to larger tensors where prior methods fail. Moreover, the structures identified by our method generalize to unseen data from the same source, enabling efficient reuse in practical applications.

Looking ahead, several directions remain open. Extending our framework to accommodate cyclic tensor networks would broaden its applicability to a wider range of physical and mathematical systems. Improving scalability for extremely high-order tensors is another promising direction.

References

Alfred V Aho and John E Hopcroft. *The design and analysis of computer algorithms*. Pearson Education India, 1974.

Doruk Aksoy, David J. Gorsich, Shravan Veerapaneni, and Alex A. Gorodetsky. An incremental tensor train decomposition algorithm. *SIAM Journal on Scientific Computing*, 46(2):A1047–A1075, 2024. doi: 10.1137/22M1537734. URL https://doi.org/10.1137/22M1537734.

Itai Arad and Zeph Landau. Quantum computation and the evaluation of tensor networks. *SIAM Journal on Computing*, 39(7):3089–3121, 2010. doi: 10.1137/080739379. URL https://doi.org/10.1137/080739379.

Mari Carmen Bañuls. Tensor network algorithms: A route map. *Annual Review of Condensed Matter Physics*, 14(1):173–191, 2023.

Terry Beyer and Sandra Mitchell Hedetniemi. Constant time generation of rooted trees. *SIAM Journal on Computing*, 9(4):706–712, 1980.

Gianluca Ceruti, Christian Lubich, and Hanna Walach. Time integration of tree tensor networks. *SIAM Journal on Numerical Analysis*, 59(1):289–313, 2021. doi: 10.1137/20M1321838. URL https://doi.org/10.1137/20M1321838.

Lieven De Lathauwer, Bart De Moor, and Joos Vandewalle. A multilinear singular value decomposition. *SIAM Journal on Matrix Analysis and Applications*, 21(4):1253–1278, 2000. doi: 10.1137/S0895479896305696. URL https://doi.org/10.1137/S0895479896305696.

Péter L Erdős and László A Székely. Applications of antilexicographic order. i. an enumerative theory of trees. *Advances in Applied Mathematics*, 10(4):488–496, 1989.

Mike Espig, Kishore Kumar Naraparaju, and Jan Schneider. A note on tensor chain approximation. *Computing and Visualization in Science*, 15:331–344, 2012.

G. Evenbly. Algorithms for tensor network renormalization. *Phys. Rev. B*, 95:045117, Jan 2017. doi: 10.1103/PhysRevB.95.045117. URL https://link.aps.org/doi/10.1103/PhysRevB.95.045117.

Glen Evenbly. A practical guide to the numerical implementation of tensor networks i: Contractions, decompositions, and gauge freedom. *Frontiers in Applied Mathematics and Statistics*, 8:806549, 2022.

Antonio Falcó, Wolfgang Hackbusch, and Anthony Nouy. Tree-based tensor formats. *SeMA Journal*, 78: 159–173, 2021.

Mehrdad Ghadiri, Matthew Fahrbach, Gang Fu, and Vahab Mirrokni. Approximately optimal core shapes for tensor decompositions. In Andreas Krause, Emma Brunskill, Kyunghyun Cho, Barbara Engelhardt, Sivan Sabato, and Jonathan Scarlett (eds.), *Proceedings of the 40th International Conference on Machine Learning*, volume 202 of *Proceedings of Machine Learning Research*, pp. 11237–11254. PMLR, 23–29 Jul 2023. URL https://proceedings.mlr.press/v202/ghadiri23a.html.

Lars Grasedyck. Hierarchical singular value decomposition of tensors. *SIAM Journal on Matrix Analysis and Applications*, 31(4):2029–2054, 2010. doi: 10.1137/090764189. URL https://doi.org/10.1137/090764189.

Johnnie Gray and Garnet Kin-Lic Chan. Hyperoptimized approximate contraction of tensor networks with arbitrary geometry. *Phys. Rev. X*, 14:011009, Jan 2024. doi: 10.1103/PhysRevX.14.011009. URL https://link.aps.org/doi/10.1103/PhysRevX.14.011009.

Zheng Guo, Aditya Deshpande, Xinyu Wang, Brian C Kiedrowski, and Alex A Gorodetsky. Hierarchical tensor network structure search for high-dimensional data. *arXiv preprint arXiv:2603.27856*, 2026.

Cécile Haberstich, A. Nouy, and G. Perrin. Active learning of tree tensor networks using optimal least squares. *SIAM/ASA Journal on Uncertainty Quantification*, 11(3):848–876, 2023. doi: 10.1137/21M1415911. URL https://doi.org/10.1137/21M1415911.

Wolfgang Hackbusch and Stefan Kühn. A new scheme for the tensor representation. *Journal of Fourier analysis and applications*, 15(5):706–722, 2009.

Stefan Handschuh. *Numerical methods in tensor networks*. PhD thesis, Dissertation, Leipzig, Universität Leipzig, 2015, 2015.

Per Christian Hansen. The truncated svd as a method for regularization. *BIT Numerical Mathematics*, 27 (4):534–553, 1987.

Meraj Hashemizadeh, Michelle Liu, Jacob Miller, and Guillaume Rabusseau. Adaptive learning of tensor network structures. *arXiv preprint arXiv:2008.05437*, 2020.

Toshiya Hikihara, Hiroshi Ueda, Kouichi Okunishi, Kenji Harada, and Tomotoshi Nishino. Automatic structural optimization of tree tensor networks. *Phys. Rev. Res.*, 5:013031, Jan 2023. doi: 10.1103/PhysRevResearch.5.013031. URL https://link.aps.org/doi/10.1103/PhysRevResearch.5.013031.

Virginia Perkins Johnson. *Enumeration Results on Leaf Labeled Trees*. PhD thesis, University of South Carolina, 2012.

Donald E Knuth. *The Art of Computer Programming: Fundamental Algorithms, Volume 1*. Addison-Wesley Professional, 1997.

Yasuaki Kobayashi, Dominik Köppl, Yasuko Matsui, Hirotaka Ono, Toshiki Saitoh, and Yushi Uno. Enumeration of ordered trees with leaf restrictions. In *From Strings to Graphs, and Back Again: A Festschrift for Roberto Grossi's 60th Birthday (2025)*, pp. 8–1. Schloss Dagstuhl–Leibniz-Zentrum für Informatik, 2025.

Tamara G. Kolda and Brett W. Bader. Tensor decompositions and applications. *SIAM Review*, 51(3): 455–500, 2009. doi: 10.1137/07070111X. URL https://doi.org/10.1137/07070111X.

Tamara G Kolda and David Hong. Stochastic gradients for large-scale tensor decomposition. *SIAM Journal on Mathematics of Data Science*, 2(4):1066–1095, 2020.

Vadim Lebedev, Yaroslav Ganin, Maksim Rakhuba, Ivan Oseledets, and Victor Lempitsky. Speeding-up convolutional neural networks using fine-tuned cp-decomposition. *arXiv preprint arXiv:1412.6553*, 2014.

Chao Li and Zhun Sun. Evolutionary topology search for tensor network decomposition. In *Proceedings of the 37th International Conference on Machine Learning*, pp. 5947–5957. PMLR, November 2020. URL https://proceedings.mlr.press/v119/li20l.html.

Chao Li, Junhua Zeng, Zerui Tao, and Qibin Zhao. Permutation search of tensor network structures via local sampling. In *Proceedings of the 39th International Conference on Machine Learning*, pp. 13106–13124. PMLR, June 2022. URL https://proceedings.mlr.press/v162/li22y.html.

Chao Li, Junhua Zeng, Chunmei Li, Cesar F. Caiafa, and Qibin Zhao. Alternating local enumeration (tnale): Solving tensor network structure search with fewer evaluations. In *Proceedings of the 40th International Conference on Machine Learning*, pp. 20384–20411. PMLR, July 2023. URL https://proceedings.mlr.press/v202/li23ar.html.

Linjian Ma, Matthew Fishman, Edwin Miles Stoudenmire, and Edgar Solomonik. Approximate contraction of arbitrary tensor networks with a flexible and efficient density matrix algorithm. *Quantum*, 8:1580, 2024.

Eva Memmel, Clara Menzen, Jetze Schuurmans, Frederiek Wesel, and Kim Batselier. Position: Tensor networks are a valuable asset for green ai. *arXiv preprint arXiv:2205.12961*, 2022.

Oscar Mickelin and Sertac Karaman. On algorithms for and computing with the tensor ring decomposition. *Numerical Linear Algebra with Applications*, 27(3):e2289, 2020.

Rachel Minster, Arvind K. Saibaba, and Misha E. Kilmer. Randomized algorithms for low-rank tensor decompositions in the tucker format. *SIAM Journal on Mathematics of Data Science*, 2(1):189–215, 2020. doi: 10.1137/19M1261043. URL https://doi.org/10.1137/19M1261043.

Simone Montangero. *Introduction to Tensor Network Methods: Numerical simulations of low-dimensional many-body quantum systems*. Springer International Publishing, 2018. ISBN 978-3-030-01408-7. doi: 10.1007/978-3-030-01409-4. URL http://link.springer.com/10.1007/978-3-030-01409-4.

Alexander Novikov, Dmitrii Podoprikhin, Anton Osokin, and Dmitry P Vetrov. Tensorizing neural networks. *Advances in neural information processing systems*, 28, 2015.

I. V. Oseledets. Tensor-train decomposition. *SIAM Journal on Scientific Computing*, 33(5):2295–2317, January 2011. ISSN 1064-8275. doi: 10.1137/090752286.

Anh-Huy Phan, Konstantin Sobolev, Konstantin Sozykin, Dmitry Ermilov, Julia Gusak, Petr Tichavskỳ, Valeriy Glukhov, Ivan Oseledets, and Andrzej Cichocki. Stable low-rank tensor decomposition for compression of convolutional neural network. In *Computer Vision–ECCV 2020: 16th European Conference, Glasgow, UK, August 23–28, 2020, Proceedings, Part XXIX 16*, pp. 522–539. Springer, 2020.

Piyush Rai, Yingjian Wang, Shengbo Guo, Gary Chen, David Dunson, and Lawrence Carin. Scalable bayesian low-rank decomposition of incomplete multiway tensors. In Eric P. Xing and Tony Jebara (eds.), *Proceedings of the 31st International Conference on Machine Learning*, volume 32 of *Proceedings of Machine Learning Research*, pp. 1800–1808, Bejing, China, 22–24 Jun 2014. PMLR. URL https://proceedings.mlr.press/v32/rai14.html.

M. Rakhuba. Robust alternating direction implicit solver in quantized tensor formats for a three-dimensional elliptic pde. *SIAM Journal on Scientific Computing*, 43(2):A800–A827, 2021. doi: 10.1137/19M1280156. URL https://doi.org/10.1137/19M1280156.

Lorenz Richter, Leon Sallandt, and Nikolas Nüsken. Solving high-dimensional parabolic pdes using the tensor train format. In Marina Meila and Tong Zhang (eds.), *Proceedings of the 38th International Conference on Machine Learning*, volume 139 of *Proceedings of Machine Learning Research*, pp. 8998–9009. PMLR, 18–24 Jul 2021. URL https://proceedings.mlr.press/v139/richter21a.html.

Joe Sawada. Generating rooted and free plane trees. *ACM Transactions on Algorithms (TALG)*, 2(1):1–13, 2006.

Farnaz Sedighin, Andrzej Cichocki, and Anh-Huy Phan. Adaptive rank selection for tensor ring decomposition. *IEEE Journal of Selected Topics in Signal Processing*, 15(3):454–463, 2021. doi: 10.1109/JSTSP.2021.3051503.

Charles Semple, Mike Steel, et al. *Phylogenetics*, volume 24. Oxford University Press on Demand, 2003.

Brent Sprangers and Nick Vannieuwenhoven. Group-invariant tensor train networks for supervised learning. *SIAM Journal on Mathematics of Data Science*, 5(4):829–853, 2023. doi: 10.1137/22M1506857. URL https://doi.org/10.1137/22M1506857.

Richard P Stanley. *Catalan numbers*. Cambridge University Press, 2015.

Gencer Sumbul, Marcela Charfuelan, Begüm Demir, and Volker Markl. Bigearthnet: A large-scale benchmark archive for remote sensing image understanding. In *IGARSS 2019-2019 IEEE International Geoscience and Remote Sensing Symposium*, pp. 5901–5904. IEEE, 2019.

Yiming Sun, Yang Guo, Charlene Luo, Joel Tropp, and Madeleine Udell. Low-rank tucker approximation of a tensor from streaming data. *SIAM Journal on Mathematics of Data Science*, 2(4):1123–1150, 2020. doi: 10.1137/19M1257718. URL https://doi.org/10.1137/19M1257718.

Makoto Takamoto, Timothy Praditia, Raphael Leiteritz, Dan MacKinlay, Francesco Alesiani, Dirk Pflüger, and Mathias Niepert. PDEBench Datasets, 2022a. URL https://doi.org/10.18419/darus-2986.

Makoto Takamoto, Timothy Praditia, Raphael Leiteritz, Dan MacKinlay, Francesco Alesiani, Dirk Pflüger, and Mathias Niepert. PDEBench: An Extensive Benchmark for Scientific Machine Learning. In *36th Conference on Neural Information Processing Systems (NeurIPS 2022) Track on Datasets and Benchmarks*, 2022b. URL https://arxiv.org/abs/2210.07182.

Ledyard R Tucker. Some mathematical notes on three-mode factor analysis. *Psychometrika*, 31(3):279–311, 1966. doi: 10.1007/BF02289464.

Frank Verstraete, Valentin Murg, and J Ignacio Cirac. Matrix product states, projected entangled pair states, and variational renormalization group methods for quantum spin systems. *Advances in physics*, 57 (2):143–224, 2008.

Steven R White. Density matrix formulation for quantum renormalization groups. *Physical review letters*, 69(19):2863, 1992.

Steven R White. Density-matrix algorithms for quantum renormalization groups. *Physical review b*, 48(14): 10345, 1993.

Johannes Wirtz. On the enumeration of leaf-labelled increasing trees with arbitrary node-degree. *arXiv preprint arXiv:2211.03632*, 2022.

Shuo Yang, Zheng-Cheng Gu, and Xiao-Gang Wen. Loop optimization for tensor network renormalization. *Physical review letters*, 118(11):110504, 2017.

Miao Yin, Huy Phan, Xiao Zang, Siyu Liao, and Bo Yuan. Batude: Budget-aware neural network compression based on tucker decomposition. *Proceedings of the AAAI Conference on Artificial Intelligence*, 36(8): 8874–8882, Jun. 2022. doi: 10.1609/aaai.v36i8.20869. URL https://ojs.aaai.org/index.php/AAAI/article/view/20869.

Shmuel Zaks. Lexicographic generation of ordered trees. *Theoretical Computer Science*, 10(1):63–82, 1980.

Junhua Zeng, Chao Li, Zhun Sun, Qibin Zhao, and Guoxu Zhou. tngps: Discovering unknown tensor network structure search algorithms via large language models (llms). In *Forty-first International Conference on Machine Learning*, 2024.

Yifan Zhang and Joe Kileel. Moment estimation for nonparametric mixture models through implicit tensor decomposition. *SIAM Journal on Mathematics of Data Science*, 5(4):1130–1159, 2023. doi: 10.1137/22M153879X. URL https://doi.org/10.1137/22M153879X.

Qibin Zhao, Guoxu Zhou, Shengli Xie, Liqing Zhang, and Andrzej Cichocki. Tensor ring decomposition. *arXiv preprint arXiv:1606.05535*, 2016.

Yu-Bang Zheng, Xi-Le Zhao, Junhua Zeng, Chao Li, Qibin Zhao, Heng-Chao Li, and Ting-Zhu Huang. Svdinstn: A tensor network paradigm for efficient structure search from regularized modeling perspective. In *Proceedings of the IEEE/CVF Conference on Computer Vision and Pattern Recognition*, pp. 26254–26263, 2024.

A Proofs

A.1 Proof of Singular Value Approximations

Definition A.1 (Subtensor)**.** Suppose $\mathcal{X} \in \mathbb{R}^{n_1 \times n_2 \times \dots n_d}$ is a d-dimensional tensor. Its subtensor $\mathcal{Y} \in \mathbb{R}^{m_1 \times m_2 \times \dots m_d}$ (written as $\mathcal{Y} \sqsubseteq \mathcal{X}$) is also a d-dimensional tensor obtained by restricting the index sets corresponding to dimension μ to m_μ elements where for all $\mu \in \{1, 2, \dots, d\}$, $m_\mu \leq n_\mu$. If $\mathcal{Y}$ is a subtensor of $\mathcal{X}$, there exists a set of binary matrices with orthonormal rows $\pi_1, \dots \pi_d$ such that $\mathcal{Y} = (\pi_1 \otimes \pi_2 \otimes \dots \otimes \pi_d)\mathcal{X}$.

Lemma A.2 (Subtensors Preservation on Permutation)**.** *Let $\mathcal{X} \in \mathbb{R}^{n_1 \times n_2 \times \dots \times n_d}$ be a d-dimensional tensor, $\mathcal{Y} \in \mathbb{R}^{m_1 \times m_2 \times \dots \times m_d}$, and $\mathcal{Y} \sqsubseteq \mathcal{X}$. If $\Pi \in \{1, \dots, d\} \to \{1, \dots, d\}$ is a permutation of the dimensions, then* $\texttt{permute}(\mathcal{Y}, \Pi(1), \dots, \Pi(d)) \sqsubseteq \texttt{permute}(\mathcal{X}, \Pi(1), \dots, \Pi(d))$.

Proof. As $\mathcal{Y} \sqsubseteq \mathcal{X}$, there exists a list of binary matrices with orthonormal rows $[\pi_\mu]_{1 \leq \mu \leq d}$ such that $\mathcal{Y} = (\pi_1 \otimes \pi_2 \otimes \dots \otimes \pi_d)\mathcal{X}$. Then, we can see that

$$\begin{aligned} & \texttt{permute}\left(\mathcal{Y}, \Pi(1), \Pi(2), \dots, \Pi(d)\right) \\ = \; & \texttt{permute}\left((\pi_1 \otimes \pi_2 \otimes \dots \otimes \pi_d)\mathcal{X}, \Pi(1), \Pi(2), \dots, \Pi(d)\right)) \end{aligned} \tag{7}$$

Since each π_μ only modifies values along the corresponding mode μ, and permutation only moves dimensions without altering values, we can move the projection outside the `permute` by reordering the projections according to the dimension permutation, and get

$$\begin{aligned} & \texttt{permute}\left((\pi_1 \otimes \pi_2 \otimes \dots \otimes \pi_d)\mathcal{X}, \Pi(1), \Pi(2), \dots, \Pi(d)\right)) \\ = \; & (\pi_{\Pi(1)} \otimes \pi_{\Pi(2)} \otimes \dots \otimes \pi_{\Pi(d)}) \; \texttt{permute}\left(\mathcal{X}, \Pi(1), \Pi(2), \dots, \Pi(d)\right) \end{aligned} \tag{8}$$

Therefore, $\texttt{permute}(\mathcal{Y}, \Pi(1), \Pi(2), \dots, \Pi(d)) \sqsubseteq \texttt{permute}(\mathcal{X}, \Pi(1), \Pi(2), \dots, \Pi(d))$ holds. □

Lemma A.3 (Subtensors Preservation on Reshape)**.** *Let $\mathcal{X} \in \mathbb{R}^{n_1 \times n_2 \times \dots n_d}$ be a d-dimensional tensor with indices $I_1, I_2, \dots, I_d$, and $\mathcal{Y} \in \mathbb{R}^{m_1 \times m_2 \times \dots m_d}$ be a d-dimensional tensor with indices $J_1, J_2, \dots, J_d$. If $\mathcal{Y} \sqsubseteq \mathcal{X}$, then for any $s \subset \{1, 2, \dots, d\}$, we have $\mathcal{X}^{(\mathcal{I}_s)} \sqsubseteq \mathcal{Y}^{(\mathcal{J}_s)}$, and vice versa.*

Proof. Since $\mathcal{Y} \sqsubseteq \mathcal{X}$, there exists binary matrices with orthonormal rows $[\pi_\mu]_{\mu \in \{1,2,\dots,d\}}$ such that

$$\mathcal{Y} = (\pi_1 \otimes \pi_2 \otimes \dots \otimes \pi_d)\, \mathcal{X} \tag{9}$$

For a set of indices $\mathcal{I}_s$, by Theorem A.2 and the associativity of tensor product, we get that

$$\mathcal{Y}^{(\mathcal{J}_s)} = \left(\bigotimes_{\mu \in s} \pi_\mu \otimes \bigotimes_{\mu \notin s} \pi_\mu \right) \mathcal{X}^{(\mathcal{I}_s)} \tag{10}$$

Therefore, we have that $\mathcal{Y}^{(\mathcal{J}_s)} \sqsubseteq \mathcal{X}^{(\mathcal{I}_s)}$.

Similarly, the property can be proved for the reverse direction by applying the above two steps in the reverse order. □

Lemma A.4 (Singular Value Upper Bound in Subtensors)**.** *Let $\mathcal{X} \in \mathbb{R}^{n_1 \times n_2 \times \dots \times n_d}$ be a d-dimensional tensor with indices $I_1, I_2, \dots, I_d$, $\mathcal{Y} \in \mathbb{R}^{m_1 \times m_2 \times \dots \times m_d}$ be a d-dimensional tensor with indices $J_1, J_2, \dots, J_d$, and $\mathcal{Y} \sqsubseteq \mathcal{X}$. Define $\sigma_i(A)$ to be the i^{th} largest singular value of a matrix A. Then, for all $s \subset \{1, 2, \dots, d\}$, if $\mathcal{I}_s = \{I_i\}_{i \in s}$ and $\mathcal{J}_s = \{J_i\}_{i \in s}$, we have $\sigma_i(\mathcal{Y}^{(\mathcal{J}_s)}) \leq \sigma_i(\mathcal{X}^{(\mathcal{I}_s)})$.*

Proof. From $\mathcal{Y} \sqsubseteq \mathcal{X}$ and Theorem A.2, we know that $\mathcal{Y}^{(\mathcal{J}_s)}) \sqsubseteq \mathcal{X}^{(\mathcal{I}_s)}$. Then, the result can be obtained by applying the Poincaré separation theorem to $\mathcal{X}^{(\mathcal{I}_s)}\big(\mathcal{X}^{(\mathcal{I}_s)}\big)^*$. □

Lemma A.5 (Singular Value Upper Bound in Truncations)**.** *Let $\mathcal{X} \in \mathbb{R}^{n_1 \times n_2 \times \dots \times n_d}$ be a d-dimensional tensor with indices $I_1, I_2, \dots, I_d$. Let $\mathcal{I}_s \subset \{I_1, I_2, \dots, I_d\}$ be a set of indices. Suppose $SVD(\mathcal{X}^{(\mathcal{I}_s)}) = U\Sigma V$. After truncation to some rank r, we get $\widetilde{\mathcal{X}}^{(\mathcal{I}_s)} = \widetilde{U}\widetilde{\Sigma}\widetilde{V}$ where $\widetilde{U} = U[:, : r]$, $\widetilde{\Sigma} = \Sigma[: r, : r]$, and $\widetilde{V} = V[: r]$. Then we have that, for all $\mathcal{I}_t \subset \{I_1, I_2, \dots, I_d\}$, if $\mathcal{I}_t \subseteq \mathcal{I}_s, \mathcal{I}_s \subseteq \mathcal{I}_t$, or $\mathcal{I}_s \cap \mathcal{I}_t = \emptyset$, then $\sigma_i(\widetilde{\mathcal{T}}^{(\mathcal{I}_t)}) \leq \sigma_i(\mathcal{X}^{(\mathcal{I}_t)})$.*

Proof. In this proof, matrices U and V can be treated as (n_s+1) and $(d-n_s+1)$ dimensional tensors where $n_s = |\mathcal{I}_s|$. The same considerations are made for $\widetilde{U}$ and $\widetilde{V}$. Due to the tree structure, we consider the following three cases of relations between $\mathcal{I}_t$ and $\mathcal{I}_s$.

- Case I: $\mathcal{I}_t = \mathcal{I}_s$. The singular values are discarded without other modification, so $\sigma_i(\widetilde{\mathcal{X}}^{(\mathcal{I}_t)}) = \sigma_i(\mathcal{X}^{(\mathcal{I}_t)})$.
- Case II: $\mathcal{I}_t \subset \mathcal{I}_s$. By the definition of matricization and SVD, we know that $\mathcal{I}_s \subset \textsc{Indices}(\widetilde{U})$. Hence, $\mathcal{I}_t \subset \textsc{Indices}(\widetilde{U})$. By Theorem A.3, Theorem A.4, and $\widetilde{U}\widetilde{\Sigma} \sqsubseteq U\Sigma$, we know that
$$\sigma_i\left(\left(\widetilde{U}\widetilde{\Sigma}\right)^{(\mathcal{I}_t)}\right) \leq \sigma_i\left((U\Sigma)^{(\mathcal{I}_t)}\right) \tag{11}$$
Therefore,
$$\sigma_i\left(\widetilde{\mathcal{X}}^{(\mathcal{I}_t)}\right) = \sigma_i\left(\left(\widetilde{U}\widetilde{\Sigma}\right)^{(\mathcal{I}_t)}\right) \leq \sigma_i\left((U\Sigma)^{(\mathcal{I}_t)}\right) = \sigma_i\left(\mathcal{X}^{(\mathcal{I}_t)}\right) \tag{12}$$
- Case III: $\mathcal{I}_s \subset \mathcal{I}_t$ or $\mathcal{I}_t \cap \mathcal{I}_s = \emptyset$. By the definition of matricization and SVD, we know that $\mathcal{I}_s \subset \textsc{Indices}(\widetilde{U})$. Hence, $\mathcal{I}_t \subset \textsc{Indices}(\widetilde{\mathcal{X}}) \setminus \textsc{Indices}(\widetilde{U}) \subset \textsc{Indices}(\widetilde{V})$. By Theorem A.3, Theorem A.4, and $\widetilde{\Sigma}\widetilde{V} \sqsubseteq \Sigma V$, we know that
$$\sigma_i\left((\widetilde{\Sigma}\widetilde{V})^{(\mathcal{I}_t)}\right) \leq \sigma_i\left((\Sigma V)^{(\mathcal{I}_t)}\right) \tag{13}$$
Therefore,
$$\sigma_i\left(\widetilde{\mathcal{X}}^{(\mathcal{I}_t)}\right) = \sigma_i\left(\left(\widetilde{\Sigma}\widetilde{V}\right)^{(\mathcal{I}_t)}\right) \leq \sigma_i\left((\Sigma V)^{(\mathcal{I}_t)}\right) = \sigma_i\left(\mathcal{X}^{(\mathcal{I}_t)}\right) \tag{14}$$

To summarize, we have $\sigma_i\left(\widetilde{\mathcal{X}}^{(\mathcal{I}_t)}\right) \leq \sigma_i\left(\mathcal{X}^{(\mathcal{I}_t)}\right)$ for all possible choices of $\mathcal{I}_t$. □

Theorem A.6 (Singular Value Upper Bound)**.** *Let $\mathcal{X} \in \mathbb{R}^{n_1 \times \cdots \times n_d}$ be a d-dimensional tensor, compressing $\mathcal{X}$ into a structure described by a dimension tree $T_{\mathcal{I}}$ of $n+1$ nodes $\mathcal{I}, \mathcal{I}_1, \mathcal{I}_2, \ldots, \mathcal{I}_n$ produces the structure $\mathcal{N}$, then for every $1 \leq i, s \leq n$, we have $\sigma_j\left({\mathcal{R}_{\mathcal{N}_i}}^{(\mathcal{I}_s)}\right) \leq \sigma_j\left(\mathcal{X}^{(\mathcal{I}_s)}\right)$ where $\sigma_j(A)$ is the j^{th} largest singular value of the matrix A, and $\mathcal{N}_i$ is the network obtained after the first i tensor decompositions specified by $T_{\mathcal{I}}$.*

Proof. By the definition of dimension trees, for every pair $1 \leq s < t \leq n$, there could only be three relations between $\mathcal{I}_s$ and $\mathcal{I}_t$: $\mathcal{I}_s \subset \mathcal{I}_t$, $\mathcal{I}_t \subset \mathcal{I}_s$, or $\mathcal{I}_s \cap \mathcal{I}_t = \emptyset$.

Suppose the network obtained after the k^{th} tensor decomposition is denoted as $\mathcal{N}_k$. The network obtained after performing the tensor decomposition on $\mathcal{N}_k$ along index set $\mathcal{I}_k$ is $\mathcal{N}_{k+1}$. Performing the split defined above is equivalent to performing a truncated SVD on ${\mathcal{R}_{\mathcal{N}_k}}^{(\mathcal{I}_k)}$. Formally, we can say that if ${\mathcal{R}_{\mathcal{N}_k}}^{(\mathcal{I}_k)} = U\Sigma V$, then ${\mathcal{R}_{\mathcal{N}_{k+1}}}^{(\mathcal{I}_k)} = \widetilde{U}\widetilde{\Sigma}\widetilde{V}$, where $\widetilde{U}$, $\widetilde{\Sigma}$, and $\widetilde{V}$ are truncated matrices of U, Σ, and V. Consequently, using Theorem A.5, we have that, for $\mathcal{I}_t \subset \{I_1, \ldots, I_d\}$ such that $\mathcal{I}_t \subseteq \mathcal{I}_s, \mathcal{I}_s \subseteq \mathcal{I}_t$, or $\mathcal{I}_s \cap \mathcal{I}_t = \emptyset$, $\sigma_i\left(\mathcal{R}_{\mathcal{N}_{k+1}}\right) \leq \sigma_i\left(\mathcal{R}_{\mathcal{N}_k}\right)$ for all possible i and k.

From the above result, we can conclude that $\sigma_i\left({\mathcal{R}_{\mathcal{N}_k}}^{(\mathcal{I}_t)}\right) \leq \sigma_i\left({\mathcal{R}_{\mathcal{N}_0}}^{(\mathcal{I}_t)}\right) = \sigma_i\left(\mathcal{X}^{(\mathcal{I}_t)}\right)$ for all valid choices of $\mathcal{I}_t$ and all possible values of i and k. □

Theorem A.7 (Upper Bound of Costs)**.** *For a data tensor $\mathcal{X}$ with indices $\mathcal{I}$, a dimension tree $T_{\mathcal{I}}$ of $n+1$ nodes $\mathcal{I}_0 = \mathcal{I}, \mathcal{I}_1, \mathcal{I}_2, \ldots, \mathcal{I}_n \subset \mathcal{I}$, and an error bound ε, let σ_{si} be the i^{th} largest singular value of $\mathcal{X}^{(\mathcal{I}_s)}$, and ς_{si} be the i^{th} largest singular value of $\hat{\mathcal{X}}^{(\mathcal{I}_s)}$ where $\hat{\mathcal{X}}$ is obtained after performing truncated SVD over $\mathcal{X}$. If $r_1, \ldots, r_n$ is a solution to the constraint solving with singular values σ_{si} for all $\mathcal{I}_s \subset \mathcal{I}$, then $r_1, \ldots, r_n$ is also a solution to the constraint solving with singular values $\varsigma_{si} \leq \sigma_{si}$.*

Proof. It is easy to see that
$$\sum_{s=1}^{n}\sum_{i>r_s}\varsigma_{si}^2 \leq \sum_{s=1}^{n}\sum_{i>r_s}\sigma_{si}^2 \leq \left(\varepsilon\|\mathcal{X}\|_F\right)^2$$
which also satisfies the linear programming constraints. □

B Example Structures

This section presents structures discovered by our tool and features the necessity of TN-SS. In each structure, square nodes denote free indices, labeled in the format of "<index name>-<index size>". Round nodes represent the constituent tensors, which are linked by contraction edges annotated with respective ranks.

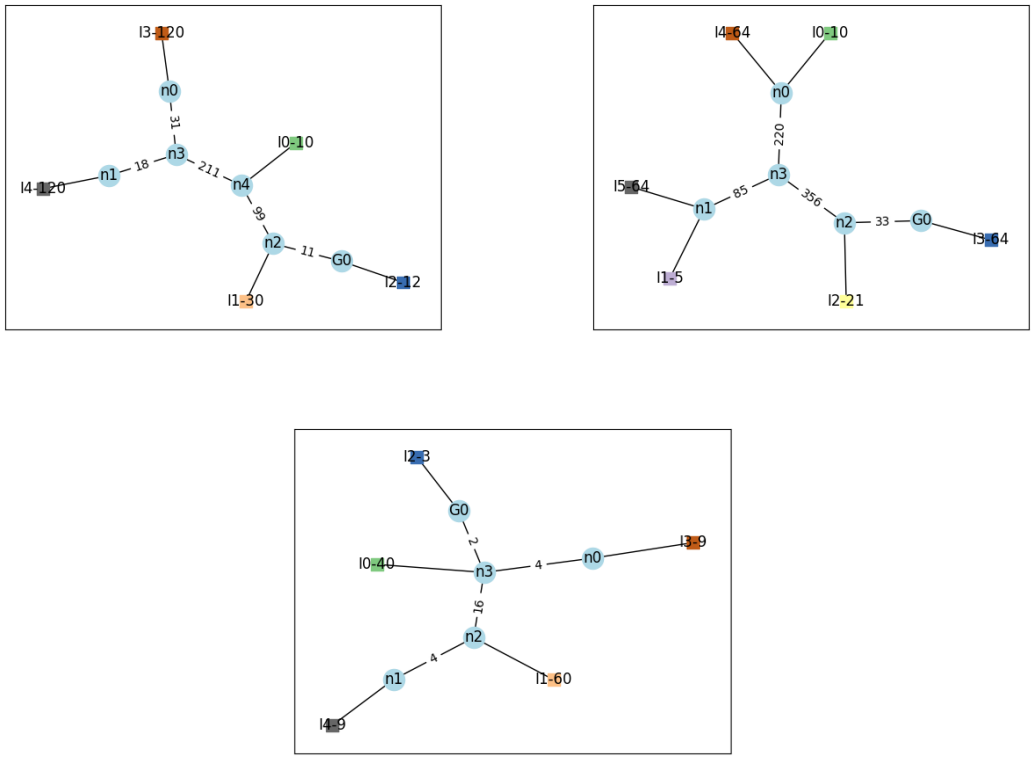

Figure 11: These structures showcase that our tool can discover non-standard structures other than TT, HT, etc. One single internal node suffices to provide good compression ratio in these cases.

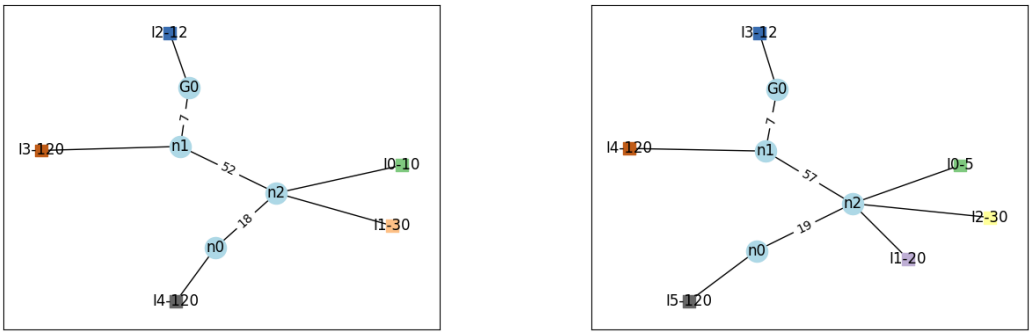

Figure 12: These two structures are similar to tensor trains but they have clustered and reordered indices, which allow them to have better compression ratios than traditional tensor trains.